Diversity of microglia

Their contribution to multiple sclerosis lesion formation

van der Poel, M.

Publication date
2020

Document Version
Other version

License
Other

Chapter 8

Gene expression profiling of multiple sclerosis pathology identifies early patterns of demyelination surrounding chronic active lesions

Debbie A.E. Hendrickx[1], Jackelien van Scheppingen[1], Marlijn van der Poel[1], Koen Bossers[2], Karianne G. Schuurman[1], Corbert G. van Eden[1], Elly M. Hol[1,3,4], Jörg Hamann[1,5]* and Inge Huitinga[1]*

[1] Neuroimmunology and [2] Neurodegeneration Research Group, Netherlands Institute for Neuroscience, Amsterdam, The Netherlands; [3] Department of Translational Neuroscience, Brain Center Rudolf Magnus, University Medical Center Utrecht, Utrecht, The Netherlands; [4] Swammerdam Institute for Life Sciences, Center for Neuroscience, University of Amsterdam, Amsterdam, The Netherlands, and [5] Department of Experimental Immunology, Academic Medical Center, University of Amsterdam, Amsterdam, The Netherlands.

*Authors contributed equally to this work

Published in *Frontiers of Immunology* 8, 1810 (2017)

Abstract

In multiple sclerosis (MS), activated microglia and infiltrating macrophages phagocytose myelin focally in (chronic) active lesions. These demyelinating sites expand in time, but at some point turn inactive into a sclerotic scar. To identify molecular mechanisms underlying lesion activity and halt, we analyzed genome-wide gene expression in rim and peri-lesional regions of chronic active and inactive MS lesions, as well as in control tissue. Gene clustering revealed patterns of gene expression specifically associated with MS and with the presumed, subsequent stages of lesion development. Next to genes involved in immune functions, we found regulation of novel genes in and around the rim of chronic active lesions, such as *NPY, KANK4, NCAN, TKTL1*, and *ANO4*. Of note, the presence of many foamy macrophages in active rims was accompanied by a congruent upregulation of genes related to lipid binding, such as *MSR1, CD68, CXCL16,* and *OLR1*, and lipid uptake, such as *CHIT1*, *GPNMB*, and *CCL18*. Except *CCL18*, these genes were already upregulated in regions around active MS lesions, showing that such lesions are indeed expanding. *In vitro* downregulation of the scavenger receptors *MSR1* and *CXCL16* reduced myelin uptake. In conclusion, this study provides the gene expression profile of different aspects of MS pathology and indicates that early demyelination, mediated by scavenger receptors, is already present in regions around active MS lesions. Genes involved in early demyelination events in regions surrounding chronic active MS lesions might be promising therapeutic targets to stop lesion expansion.

Introduction

Multiple sclerosis (MS) is a neurological disease characterized by focal demyelinating lesions in the central nervous system, leading to a variety of symptoms, including problems with motor control, numbness or tingling sensation, cognitive problems, depression, and fatigue. Both genetic and environmental factors play a role in the onset and progression of MS [reviewed in Ref.[1,2]]. Demyelination in MS is mediated by activated microglia and infiltrating macrophages, and in brains and the spinal cord of MS patients, both (chronic) active lesions and inactive scars are found. It is not clear why MS lesions are active demyelinating and which mechanisms contribute to the halt of lesion activity.

Depending on the level of demyelination and microglia/macrophage activation, MS lesions are characterized as active, chronic active, or inactive[3,4]. Active lesions contain lipid-laden microglia/macrophages throughout the lesions, while chronic active MS lesions have a demyelinated sclerotic core, surrounded by a rim of foamy microglia/macrophages. A recent magnetic resonance imaging study showed that chronic active lesions expand in time[5], and it is thought that at some point, active lesions turn into inactive sclerotic scars. Moreover, we found that chronic active lesion load correlates with fast progression of the disease, illustrating the clinical implications of lesion expansion (Luchetti *et al.*, submitted).

Identification of gene expression in presumed, subsequent stages of MS lesions will increase insight into the molecular mechanisms related to lesion activity and halt. Gene expression profiling studies so far, on tissue blocks containing MS lesions from limited numbers (3–5) of MS patients per study, showed overall upregulation of pro-inflammatory pathways[6–10] and oxidative injury[11]. One gene expression analysis of normal appearing white matter (NAWM) in MS demonstrated upregulation of genes associated with immunosuppression and protective mechanisms, but also pro-inflammatory mechanisms, suggesting a state of low-level inflammation and an unsteady balance[12,13].

Previously, we analyzed differential gene expression between rims and regions surrounding chronic active and inactive MS lesions in substantial numbers of well-characterized MS brain donors by quantitative polymerase chain reaction (qPCR) and identified downregulation of macrophage inhibitory molecules around chronic active lesions[13]. In this follow-up study, we set out a hypothesis-free microarray approach to study gene expression in rims and peri-rim regions of and around chronic active and inactive MS lesions from 15 MS patients and white matter (WM) of 10 matched control subjects. We identified gene expression specifically related to MS and to the assumed, subsequent stages of lesion development. Strikingly, genes connected with lipid binding and uptake were increased in the rim and peri-rim of chronic active lesions.

Materials and Methods

Human tissue

Post-mortem human brain tissue was provided by the Netherlands Brain Bank (NBB, Amsterdam, The Netherlands; www.brainbank.nl). Informed consent was obtained from donors for brain

autopsy and the use of tissue and clinical information for research purposes. At the time of death, 12 patients had relapsing-remitting course of the disease, 1 had a primary-progressive disease course, and for 2, the disease course could not be determined. MS diagnosis was confirmed post-mortem by a neuropathologist. One-way ANOVA analysis (Kruskal–Wallis test) showed no significant difference in age, post-mortem delay, or pH of cerebrospinal fluid (CSF) between the groups. Detailed donor characteristics are provided in **Table 1**; **Table S1** in Supplementary Material.

Tissue dissection and RNA isolation

Cryostat sections were stained for myelin proteolipid protein (PLP; Serotec, Oxford, UK) and HLA-DP/Q/R (DAKO, Glostrup, Denmark) to assess MS lesion activity. Chronic active MS lesions were characterized by a sclerotic hypocellular demyelinated core, surrounded by a clear distinct rim of foamy HLA-positive macrophages[14]. Inactive MS lesions were sclerotic demyelinated lesions without activated macrophages[3]. Frozen chronic active and inactive MS lesions were cut in 20 μm sections using a cryostat and mounted on PALM MembraneSlides (PALM Microlaser Technologies, Munich, Germany). Every fifth to seventh section was stained with Sudan Black to confirm the lesion was still present and to facilitate dissection. Furthermore, every first and last section was stained for PLP and HLA-D/Q/R to assure continuous lesion activity. The rim and peri-lesional (PL)-NAWM were dissected by laser dissection microscopy and stored in ice-cold TRIsure (Bioline, London, UK). Control tissue was dissected inside the cryostat using a pre-chilled scalpel and also stored in ice-cold TRIsure. After addition of chloroform and centrifugation, the aqueous phase was removed and mixed with an equal volume of 70% RNase-free ethanol. Samples were then applied to an RNeasy Mini column (Qiagen, Valencia, CA, USA) and further processed according to manufacturer's instructions. RNA yield was determined using a NanoDrop ND-1000 spectrophotometer (NanoDrop Technologies, Wilmington, DE, USA), and quality was assessed on a Bioanalyzer 2100 (Agilent Technologies, Palo Alto, CA, USA). Only samples with RNA integrity number (RIN) values ≥5 were included. In total, 7 chronic active MS lesions, 8 inactive MS lesions, and WM of 10 control donors were included in this study. RIN values of control donors were significantly higher than of any of the MS lesion subareas. However, there was no difference in RIN value between the rim of chronic active versus the rim of inactive MS lesions, or the PL-NAWM of chronic active versus the PL-NAWM of inactive MS lesions.

Table 1 | Donor characteristics per group

Tissue type	Lesion area	Sex	Age	pH	PMD	RIN
Chronic active	Rim	2 M / 5 F	49.4 ± 8.6	6.42 ± 0.17	8:24 ± 1:55	6.39 ± 0.67
	PL-NAWM					6.43 ± 0.33
Inactive	Rim	2 M / 6 F	63.3 ± 11.7	6.43 ± 0.21	9:03 ± 0:45	5.79 ± 0.62
	PL-NAWM					6.16 ± 0.50
Control		3 M / 7 F	59.7 ± 10.4	6.67 ± 0.35	8:23 ± 2:51	7.42 ± 0.67
One-way ANOVA			p=0.1351	p=0.3941	p=0.6958	p=0.0003

Age = age at death (years); F = female; M = male; pH = pH of CSF; PL-NAWM = perilesional normal-appearing white matter; PMD = post-mortem delay (h:min); RIN = RNA integrity number. Data are represented as mean ± SD.

Sample preparation and microarray hybridization

The Low Input Quick Amp Labeling Kit (Agilent Technologies) was used for sample amplification and fluorescent labeling according to manufacturer's instructions. Briefly, 100 ng experimental RNA input and 50 ng reference pool RNA input was used for linear amplification and fluorescent labeling. The reference pool RNA was extracted from snap-frozen tissue dissected from a diversity of anatomical regions from control and MS brains, including MS lesions and NAWM, as well from tonsil. Experimental samples were labeled with Cy5-CTP, and the reference pool was labeled with Cy3-CTP (Perkin Elmer, Waltham, MA, USA). The cRNA samples were purified using RNeasy mini columns (Qiagen), and quantity and labeling efficiency (specific activity) was determined on a NanoDrop.

Prior to hybridization, 825 ng Cy3- and Cy5-labeled cRNA samples were fragmented by 30 min incubation at 60°C in 1× fragmentation buffer (Agilent Technologies). Each time, one Cy5-labeled experimental sample and one Cy3-labeled reference pool sample were hybridized to an Agilent Human Gene Expression 4×44K v2 Microarray (Part Number G4845A) for 17 h at 65°C in a rotating hybridization chamber. Arrays were washed in 6× saline sodium phosphate-EDTA (SSPE)/0.005% N-lauroylsarcosine (Sigma-Aldrich, St. Louis, MO, USA) for 5 min, then in 0.06× SSPE/0.005% N-lauroylsarcosine for 1 min, and finally in acetonitrile (Sigma-Aldrich) for 30 s. After drying in a nitrogen flow, arrays were scanned using an Agilent DNA Microarray Scanner at 5 mm resolution and 100% photomultiplier tube setting. Microarray scans were quantified using Agilent Feature Extraction software (version 9.5.3.1).

Microarray normalization and single gene analysis

Common reference cRNA was co-hybridized to every microarray slide to allow for accurate comparison of expression levels across different cDNA microarray experiments. In this way, a ratio between the experimental and reference material could be calculated for every spot, and expression levels across different hybridizations could be compared. Raw expression data were imported into the R statistical processing environment using the LIMMA package in Bioconductor.2 All features for which one or more foreground measurements were flagged as saturated or as a non-uniformity outlier by the feature extraction software were excluded from further analysis. As overall background levels were very low, no background correction was performed. Data within an array were normalized using loess (LIMMA), which was followed by a between-array normalization using the Gquantile algorithm in LIMMA. Subsequently, for probes that mapped to the same gene, the average M- and A-value of those probes were used for further analyses. Differential gene expression was assessed using a single channel analysis on the M-values using Bayesian statistics in LIMMA. Three contrasts were investigated: (I) chronic active rim vs. inactive rim, (II) chronic active PL-NAWM vs. inactive PL-NAWM, and (III) chronic active PL-NAWM vs. control. Correction for multiple testing was performed with the Benjamini–Hochberg algorithm. Genes with a p-value <0.05 were considered significant.

Cluster analysis of gene expression data in different stages of lesion activity

In order to follow the expression of individual transcripts in different presumed subsequent stages of lesion activity and demyelination, expression profiles were constructed from regions that represent no pathology (control NAWM), the early events in demyelination (PL-NAWM around chronic active MS lesions), fully active demyelination (rim of chronic active MS lesions), halt of demyelination (rim of inactive MS lesions), and absence or suppression of early demyelination (PL-NAWM of inactive lesions, **Figure 1**). The NIA Array Analysis software was used to find these clusters of genes showing the same expression pattern across the different subareas studied[15]. The intensity values of all genes were used as input. The NIA Array Analysis software uses ANOVA (with error variance averaging and Benjamini correction for false discovery rate) to test statistical significant genes. Only significant genes were displayed.

Gene ontology overrepresentation analysis

The overrepresentation of specific GO terms within the different clusters was analyzed using GOstat with the goa_human database (minimum path length of 3 and Benjamini correction for false discovery rate). All statistical significant genes per cluster were used as input, and all genes measured on the array were used as the background set of genes.

cDNA synthesis and qPCR

Reverse transcription was performed in a reaction mixture of 10 µl containing 100 ng RNA and gDNA Wipeout Buffer, incubated for 2 min at 42°C, and Quantiscript® Reverse Transcriptase, Quantiscript Buffer, and room temperature (RT) Primer Mix (Qiagen Benelux, Venlo, The Netherlands), incubated for 15 min at 42°C. RT transcriptase was inactivated by incubation for 3 min at 95°C.

Primer pairs for real-time qPCR were designed using the NCBI primer basic local alignment search tool; see **Table S2** in Supplementary Material for the primer pairs used in this study. Specificity was tested on cDNA derived from brain or laser dissection microscopy-isolated test brain tissue of MS donors and control donors by assessment of the dissociation curve and PCR product, as determined by size fractionation on an 8% sodium dodecyl sulfate polyacrylamide gel electrophoresis gel.

Quantitative polymerase chain reaction reactions were performed with SYBR Green PCR Master Mix (Applied Biosystems, Foster City, CA, USA) with samples containing equal cDNA concentrations of 2–3.5 ng total RNA per reaction. Analysis was performed according to the manufacturer's protocol and the ABI Prism 7300 Sequence Detection System (Applied Biosystems). Target genes were normalized to the geometric mean of glyceraldehyde 3-phosphate dehydrogenase (*GAPDH*), tubulin α (*TUBA1A*), or elongation factor 1 alpha (*EEF1A1*) mRNA expression, which did not differ significantly between the different groups studied. Fold differences were calculated using the $2^{-\Delta\Delta CT}$ method[16].

Immunohistochemistry

Tissue of donors used for detection of protein expression are displayed in **Table 1**. For CHIT1, frozen sections (20 μm) of both active and inactive MS lesions and control tissue were fixed for 20 min in 4% paraformaldehyde. For GPNMB, OLR1, and ANO4, paraffin-embedded sections (6 μm) of both active and inactive MS lesions and control tissue were deparaffinized with xylene and rehydrated, and antigen retrieval was performed by incubation in tris-buffered saline (TBS) for GPNMB and OLR1 and in citrate buffer at pH6 for ANO4 (microwave, 10 min at 700 W). Aspecific binding was blocked by incubation in 10% normal horse serum (NHS) for 30 min at RT, followed by incubation with primary antibodies directed at CHIT1 (NBP1-84490, 1:20; Novus Biologicals, Abingdon, UK), GPNMB (MAB15501, 1:200; R&D Systems, Oxon, UK), OLR1 (H00004973-D01, 1:500; Abnova, Taoyuan City, Taiwan), or ANO4 (19488-1-AP, 1:50; Proteintech, Manchester, UK) diluted in incubation buffer (0.25% gelatin and 0.5% Triton-X in TBS, pH 7.6), for 1 h at RT. Immunoreactivity was visualized by using avidin–biotin complex (Vector PK-6100, Burlingame, CA, USA), followed by diaminobenzidine chromogenic substrate system (EnVision, DAKO) for CHIT1 or immediately by using the EnVision detection system (Dako) for GPNMB and OLR1. Sections were counterstained by 0.025% cresyl violet and embedded in Entellan. Immunoreactivity was examined using a Zeiss Axioskop 9801 light microscope (Zeiss, Oberkochen, Germany).

Cell culture and gene silencing

The human monocytic cell line THP-1 was cultured in Roswell Park Memorial Institute (RPMI) glutaMAX medium containing 10% fetal calf serum and 1% penicillin/streptomycin. For flow cytometric or PCR analysis, cells were cultured in plates coated with poly(2-hydroxyethyl methacrylate), otherwise known as hydron (Sigma-Aldrich), to prevent adherence. For immunocytochemistry, cells were cultured on glass coverslips. Cells were differentiated into macrophage-like cells by stimulation with 160 nM phorbol 12-myristate 13-acetate (PMA) for 24 h, followed by another 24 h culture in normal medium. To measure unlabeled myelin uptake over time, cells were stimulated with 8 nM PMA for 48 h, followed by 5 days culture in normal medium.

Gene silencing was performed using locked nucleic acid (LNA) oligonucleotides, designed using the siDesign center of Thermo Scientific and synthesized by Santaris Pharma A/S (Hørsholm, Denmark). The following oligonucleotide sequences and concentrations were used: *MSR1* (CCCGTGAGACTTTGAG; 2 μM), *CXCL16* (AGTGAGCTCTTTGTCC; 5 μM), *OLR1* (CTCATTCAGCTTCCGA; 2.5 μM), and *CD68* (AACTGAAGCTCTGCCC; 2.5 μM). The 16-mers contained three LNA moieties at both termini (underlined). Oligonucleotide uptake was achieved without any additives, through a process called gymnosis[17]. Differentiated cells were incubated with the oligonucleotides for 6 days before myelin uptake was tested. For inhibition of a broad spectrum of scavenger receptors, cells were pre-incubated with 100, 500, or 1,000 μg/ml fucoidan (Sigma, Zwijndrecht, The Netherlands) for 45 min before myelin was added.

Phagocytosis assay

Myelin was isolated from the myelin-containing fraction of post-mortem human brain tissue collected after Percoll gradient separation. Unlabeled myelin was used to measure myelin uptake over time, and myelin stained with the pH sensitive dye pHrodo red (Invitrogen) was used for gene silencing experiments to visualize uptake in the lysosomal compartment, as described recently[18].

Free floating THP-1 macrophages were incubated with 12.5 μg pHrodo-labeled MS or control myelin per 80,000 cells for 24 h. After incubation, the cells were collected and washed in cold phosphate-buffered saline (PBS) with 1% bovine serum albumin for quantification of myelin uptake by flow cytometry after gene silencing. Expression of *CHIT1* and *GPNMB* was determined after incubation with unlabeled 12.5 μg MS or control myelin for 1, 2, or 5 days in duplo. After 5 days, the medium was refreshed and cells were incubated for 80 more hours in normal medium. Harvested cells were stored in TRisure and gene expression of *CHIT1* and *GPNMB* was analyzed by qRT-PCR.

For flow cytometric analysis, cells were incubated with the viability dye eFluor 780 (eBiosciences; 1:2,000) for 30 min on ice. Uptake of pHrodo-labeled myelin was measured on a FACSCanto machine (BD Biosciences) and analyzed using FlowJo 7.6 software (**Figure S1** in Supplementary Material). Phagocytosis was expressed as percentage of live cells that took up myelin and as geomean fluorescence intensity of the pHrodo signal indicating the total amount of myelin phagocytosed.

For immunocytochemical analysis, cells on glass coverslips were fixed in 4% paraformaldehyde for 15 min and washed with PBS. Aspecific binding was blocked by incubation in 10% NHS for 30 min at RT, followed by incubation with the primary antibody directed at MSR1 (MAB1716, 1:100; Abnova), diluted in incubation buffer (0.25% gelatin and 0.5% Triton-X in TBS pH 7.6), O/N at 4°C. The next day, cells were washed and incubated with the fluorescently labeled secondary antibody (donkey anti-mouse Cy3 conjugated antibody, 1:1,000; Millipore) in incubation buffer with Hoechst 1:1,000 for nuclear staining for 1 h at RT. Coverslips were then washed in PBS and demineralized water and embedded in mounting medium (0.605 g Tris pH 8.5, 12.5 ml glycerol 100%, and 5 g Mowiol; EMD Chemicals, Gibbstown, NJ, USA).

Fluorescent images were taken on an Axiovert microscope (Zeiss) with Neoplanfluor objectives using an Exi Aqua Bioimaging microscopy camera (QImaging, Surray, BC, Canada) and ImagePro software (MediaCybernetics, Bethesda, MD, USA).

Statistical analysis

Statistical analysis of qPCR validation and cell culture experiments was performed using GraphPad Prism version 6 software (GraphPad Inc., La Jolla, CA, USA). The non-parametric Kruskal–Wallis test, followed by post hoc comparisons (Mann– Whitney U test) was performed to assess the regulation of genes of interest and the effect of gene silencing and addition of fucoidan. Differences between THP-1 cells incubated with MS, control, or no myelin over time were assessed with One-way ANOVA, followed by Tukey's multiple comparisons test. *P*-values <0.05 were considered significant.

Results

Identification of genes that show significantly altered expression in different MS lesion subregions

Using laser-based microdissection, we isolated the rim and PL region of and around chronic active and inactive MS lesions from 15 MS patients and WM of 10 matched control subjects and analyzed differences in gene expression using Agilent Human Gene Expression 4×44K v2 microarrays. The following comparisons were made: (I) chronic active rim *vs*. inactive rim, (II) chronic active PL-NAWM *vs*. inactive PL-NAWM, and (III) chronic active PL-NAWM *vs*. control WM (**Figure 1**; Roman numbers). In comparison I, we expected to find genes involved in either active demyelination (upregulated in chronic active rim) or cessation of demyelination (upregulated in inactive rim). Genes in comparison II were expected to be involved in early demyelination and expansion of lesions (upregulated in chronic active PL-NAWM) or the prevention and exhaustion of lesion expansion (upregulated in inactive PL-NAWM). Finally, comparison III was expected to show genes involved in initial lesion onset (either protective genes that are downregulated or inflammatory or phagocytic genes that are upregulated in chronic active PL-NAWM). This resulted in a total of 1,251 significantly regulated genes in comparison I, 587 genes in comparison II, and 3,434 genes in comparison III, with a p-value< 0.05. For an overview of the top 50 significantly upregulated and downregulated genes per comparison, see **Figure 2**; **Tables S3A-F** in Supplementary Material.

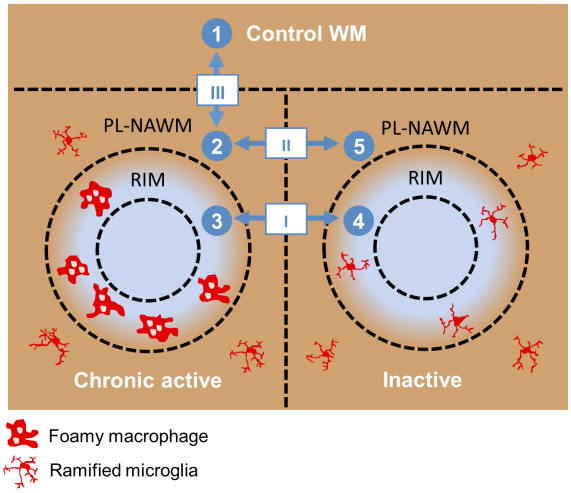

Figure 1 | Schematic overview of the different microarray analyses done. Roman numbers indicate direct comparisons. (I) chronic active rim *vs*. inactive rim, (II) chronic active peri-lesional (PL)-normal appearing white matter (NAWM) *vs*. inactive PL-NAWM, and (III) control *vs*. chronic active PL-NAWM. Arabic numbers indicate the sequence used for cluster analysis. (1) Control white matter (WM), (2) chronic active PL-NAWM, (3) chronic active rim, (4) inactive rim, (5) inactive PL-NAWM.

Cluster analysis

A cluster analysis was performed using the NIA Microarray Analysis Software to visualize gene expression during the presumed, subsequent stages of MS lesion activity and halt. The following sequence was chosen as input: (1) control WM, (2) chronic active PL-NAWM, where initial events in demyelination may be present in case the chronic active lesion was expanding, (3) chronic active rim, where active demyelination is ongoing, (4) inactive rim, where earlier demyelination has ceased, and (5) inactive PL-NAWM, where lesion progression has stopped (**Figure 1**; Arabic numbers). This gene cluster analysis revealed six specific patterns of gene expression between the subgroups tested

(**Figure 3**). Some genes were generally expressed lower (cluster 1) or higher (cluster 2) in all lesion subregions, compared to control tissue. The other four patterns followed the presumed sequence of MS lesion development with a peak of gene expression around chronic active lesions (cluster 3), a peak of gene expression in the rim of chronic active lesions (cluster 4), low gene activity around active rims, but high expression in active rims and (peri)-rims of inactive lesions (cluster 5), and high gene expression in and around inactive lesions, but low activity in active rims (cluster 6).

The GO of the specific gene expression clusters was analyzed by GOstat[19] (**Table S4** in Supplementary Material). The GO shows which gene functions are overrepresented within the groups studied, compared to all genes measured on the microarray. The most robust associations (i.e., with many GO terms changed) were found in cluster 2 and 4. In cluster 2, with overall high expression in MS, genes involved in immune functions were overrepresented, which is in line with MS being an inflammatory disease. In cluster 4, with highest expression in the active rim, genes involved in immune response/antigen presentation and cellular compartmentation, e.g., membrane and lysosome, were overrepresented, corresponding with the process of demyelination. In cluster 1, cluster 5, and cluster 6, associations were less robust. In cluster 1, with overall low expression in MS, various cellular functions linked with homeostasis were overrepresented. In cluster 5, with high expression in active rims and (peri)-rims of inactive lesions, but low activity in peri-rims of chronic active lesions, genes involved in extracellular matrix and/or collagen synthesis were overrepresented. In cluster 6, with high expression in and around inactive lesions, but low activity in active rims, sterol biosynthesis was overrepresented. The number of genes that fell within cluster 3 (n = 3) was too low for the GO analysis. The GO also showed a shift in the expression location of overrepresented genes from the plasma membrane to the lysosomal membrane from comparison II to comparison I (data not shown). Furthermore, processes involved in lipid metabolism were overrepresented in comparison I (data not shown).

Selection of genes of interest

Genes of interest were selected based on their regulation between the subgroups (direct comparisons) and their expression pattern in the cluster analysis, with a specific interest of genes regulated peri-lesionally around chronic active lesions. *CHIT1* (chitinase 1), *GPNMB* (glycoprotein non-metastatic melanoma protein B), and *CCL18* (C–C motif chemokine ligand 18) were the most upregulated genes in comparison I. *CHIT1* showed the highest expression in the rim of chronic active in the rim of inactive MS lesions (**Figure 2**). *CHIT1* was also slightly upregulated in the PL-NAWM of chronic active MS MS lesions, with a 10.2-fold change, compared to the expression lesions, compared to the PL-NAWM of inactive MS lesions (fold change of 2.0). *GPNMB* and *CCL18* showed a peak in expression in the rim of chronic active MS lesions, compared to the rim of inactive MS lesions, with a fold change of 8.0 and 6.8, respectively (**Figure 2**). Moreover, *GPNMB* was most highly induced around chronic active lesions compared to control tissue (fold change of 7.1) in comparison III.

Myelin recognition and uptake requires the presence of dedicated receptors at the surface of microglia/macrophages. We previously reported selective upregulation of scavenger receptors in and around demyelinating areas in MS[14]. Congruently, genes upregulated in the rim of chronic active

MS lesions compared to the rim of inactive MS lesions (comparison I) included the scavenger receptors *OLR1* [oxidized low-density lipoprotein receptor 1, also known as lectin-type oxidized LDL receptor 1 (LOX-1)], *CD68* (cluster of differentiation 68), *MSR1* [macrophage scavenger receptor 1, also known as scavenger receptor AI/II (SR-AI/II)], and *CXCL16* (C-X-C motif chemokine ligand 16) (fold change of 2.8–1.8) (**Figure 2**). *OLR1, CD68,* and *MSR1* were also upregulated in the PL-NAWM of chronic active MS lesions, compared to the PL-NAWM of inactive MS lesions and to control tissue (comparisons II and III), indicating that these molecules may be involved in initial demyelination. All scavenger receptors showed the highest expression in the rim of chronic active MS lesions.

Comparison I: chronic active rim vs inactive rim				Comparison II: chronic active PL-NAWM vs inactive PL-NAWM				Comparison III: chronic active PL-NAWM vs control			
Gene symbol	FC	FC	Gene symbol	Gene symbol	FC	FC	Gene symbol	Gene symbol	FC	FC	Gene symbol
CHIT1	10.2	0.3	HBB	NPY	5.9	0.3	LOC100289290	GPNMB	7.1	0.1	AL050203
GPNMB	8.0	0.3	HBD	GABRA1	3.9	0.3	CRLF1	SERPINA3	7.0	0.1	DEFA3
CCL18	6.8	0.3	CRLF1	SYNPR	3.8	0.3	IGJ	APOC1	6.3	0.2	LOC100132168
ACP5	6.4	0.3	ABCA6	NPTX1	3.7	0.3	ABCA6	VIM	5.1	0.2	MYH7B
PKD2L1	5.7	0.3	KANK4	VSNL1	3.7	0.3	KANK4	MSR1	4.8	0.2	ENST00000443002
HLA-DQA1	4.7	0.4	RNU2-2	OPALIN	3.6	0.4	ENST00000392423	CD44	4.5	0.2	CPAMD8
FCGR2B	4.6	0.4	DHCR24	SYN2	3.5	0.4	C21orf130	OLR1	4.2	0.3	YJEFN3
CFD	4.5	0.4	TSPAN8	SNAP25	3.4	0.4	ARRDC4	PALLD	4.1	0.3	ATPGD1
APOC1	4.4	0.4	ENST00000392423	CREG2	3.3	0.4	ENST00000313339	CHI3L1	4.0	0.3	CIRBP
CXCR4	4.1	0.5	SQLE	GABRB2	3.2	0.4	TSPAN8	ANXA1	3.9	0.3	KCNQ2
PLA2G7	4.0	0.5	ENST00000313339	SYT4	3.1	0.4	TTN	EMP1	3.8	0.3	A_33_P3253832
HS3ST2	4.0	0.5	RBM11	SYT13	3.1	0.4	ARMC3	S100A10	3.8	0.3	ABCA2
IFI30	3.6	0.5	RNU1-5	* NCAN	2.7	0.5	RBM11	RFTN1	3.6	0.3	CITED4
CAPG	3.2	0.5	FSTL5	FGF13	2.6	0.5	FSTL5	IFI30	3.5	0.3	UNC84B
RAB42	3.0	0.5	RMRP	GDA	2.6	0.5	DHCR24	ANO6	3.5	0.3	LOC283999
MS4A7	3.0	0.5	WIF1	SV2B	2.5	0.5	C15orf51	CP	3.5	0.3	LIPE
ITGAX	2.9	0.5	TTN	CADPS	2.5	0.5	HYDIN	ABCA1	3.4	0.3	ENST00000369123
AMICA1	2.9	0.5	RELN	BASP1	2.5	0.5	ANKRD20B	FPR3	3.3	0.3	CERCAM
DENND2D	2.9	0.5	LOC728449	MAL2	2.5	0.5	POU2AF1	PLA2G7	3.3	0.3	ENST00000293201
OLR1	2.9	0.5	TNFRSF21	GNLY	2.5	0.5	MTUS1	CD84	3.3	0.3	LOC349114
ALOX5AP	2.8	0.5	LOC100133402	KCNC2	2.5	0.5	PPEF1	TGFB2	3.1	0.3	KLC2
FGR	2.8	0.5	C21orf130	KCNMA1	2.4	0.5	MBOAT1	FRMD3	3.1	0.3	ENST00000405068
CD68	2.8	0.5	LOC100290344	CDH18	2.4	0.5	RELL1	S100A6	3.1	0.3	DNAJB2
IRF5	2.8	0.5	PDE11A	TNFRSF12A	2.3	0.5	DPYSL5	NSL1	3.0	0.3	ADORA1
MSR1	2.8	0.5	SNORA28	RGS7BP	2.3	0.5	LOC728449	LGALS3	3.0	0.3	LOC340335
ASCL2	2.8	0.5	ANKRD20B	CBLN2	2.3	0.5	HN1L	SAMSN1	3.0	0.3	CCDC85B
HLA-DMB	2.8	0.5	LDLR	ENC1	2.2	0.5	TNFRSF21	MS4A7	3.0	0.3	A_33_P3209176
SLC7A7	2.8	0.5	ALAS2	PRICKLE1	2.2	0.5	ANKRD18A	COLEC12	2.9	0.3	ENST00000371623
TNFAIP2	2.7	0.5	KLK6	MRAP2	2.2	0.5	SNX24	DTNA	2.9	0.3	PCBP4
BCL2A1	2.7	0.5	RAPGEF5	HOPX	2.2	0.6	SPARC	FGF2	2.9	0.3	STMN4
HLA-DRB5	2.7	0.5	MBP	ELMOD1	2.2	0.6	GOLGA8E	NCF2	2.9	0.3	CMTM5
ADORA3	2.7	0.5	F5	FGF12	2.2	0.6	LOC283481	SPP1	2.9	0.3	TMEM63A
SLC47A1	2.7	0.5	HAPLN2	CHI3L1	2.1	0.6	AK058117	MAFB	2.8	0.3	DAO
MX2	2.7	0.5	ABCA8	NCEH1	2.1	0.6	ENST00000423618	SORBS1	2.8	0.3	HMX1
S100A11	2.6	0.5	NIPAL4	GABRB3	2.1	0.6	TTC25	DST	2.8	0.3	A_33_P3277805
NCF2	2.6	0.5	CDKN1C	CD83	2.1	0.6	LOC645321	PTPRC	2.8	0.3	LTBP3
CD83	2.6	0.5	GDF10	ISG15	2.1	0.6	MRO	DAAM1	2.8	0.3	DOHH
FCGR2C	2.6	0.5	MOBP	LRRN3	2.1	0.6	KLK6	DDR2	2.8	0.3	FTCD
ENST00000424686	2.6	0.5	HN1L	ALOX5AP	2.1	0.6	LOC284232	TRIM34	2.7	0.3	ST3GAL4
HLA-DQA2	2.6	0.5	ENPP6	ADORA3	2.1	0.6	RND2	S1PR3	2.7	0.3	FLJ45445
SIGLEC8	2.6	0.5	LOC283713	OLR1	2.1	0.6	LRAT	DENND2D	2.7	0.3	PAQR6
ENST00000412049	2.6	0.5	DPYSL5	* ANO4	2.1	0.6	NIPAL4	TPST1	2.6	0.3	tcag7.907
CCRL2	2.5	0.5	INSIG1	GAP43	2.1	0.6	DNAJC15	MAN2A1	2.6	0.3	PNPLA7
MS4A4A	2.5	0.6	LOC100008587	GFRA2	2.1	0.6	CCDC11	CNN3	2.6	0.3	LONP1
FCER1G	2.5	0.6	TMEM125	TMEM233	2.1	0.6	HAPLN2	MAN1C1	2.6	0.3	SBF1
HPSE	2.5	0.6	TMEM144	MX1	2.0	0.6	OFD1	CCRL2	2.6	0.3	ENST00000401999
LAPTM5	2.5	0.6	SPOCK3	CNR1	2.0	0.6	MAP4	EVI2B	2.5	0.3	HES6
LSP1	2.5	0.6	RHBDL2	BEX1	2.0	0.6	CFH	LIMS1	2.5	0.3	AGAP3
HLA-DMA	2.5	0.6	ERMN	GPR98	2.0	0.6	DNAH12	GPR65	2.5	0.3	ATP6V0E2
KLHL6	2.5	0.6	DMBT1	IFI30	2.0	0.6	MOBKL2B	SLC5A3	2.5	0.3	MVD

Figure 2 | Top 50 significantly upregulated and downregulated genes in multiple sclerosis lesion subregions. For a description of the comparisons, see Figure 1 and text. Upregulated genes are indicated in red and downregulated genes are indicated in blue. Genes colored and marked in bold have been selected for further investigation. Genes expressed in cluster 3 are marked by an asterisk. Further details on the genes and *p*-values are provided in Tables S3A–F in Supplementary Material. FC= fold change.

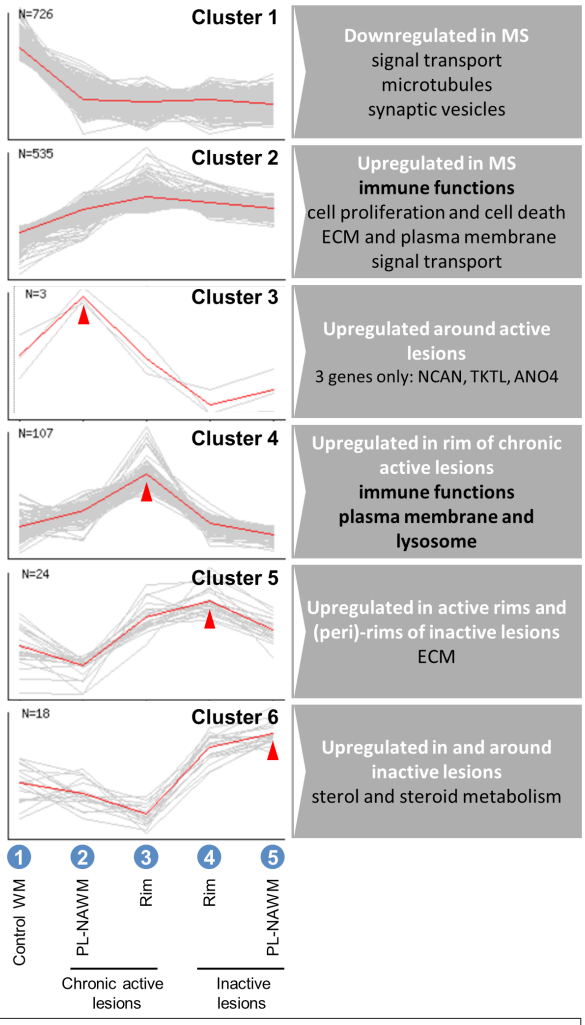

Figure 3 | Cluster analysis of gene expression in and around multiple sclerosis (MS) lesions. Analysis was done with the sequence: (1) control white matter (WM), (2) chronic active perilesional (PL)-normal appearing white matter (NAWM), (3) chronic active rim, (4) inactive rim, (5) inactive PL-NAWM (also shown in Figure 1), which resulted in six different expression patterns, representing overall differences between control and MS (clusters 1 and 2), specific upregulation around expanding chronic active lesions (cluster 3), specific upregulation in active rims (cluster 4), upregulation in active rims and (peri)-rims of inactive lesions (cluster 5), or upregulation in and around inactive lesions (cluster 6). N indicates the number of significantly regulated genes within a cluster.

Three other molecules of interest were *CXCR4* (C-X-C motif chemokine receptor 4), *NPY* (neuropeptide Y), and *KANK4* (KN motif and ankyrin repeat domains 4). The chemokine receptor *CXCR4* was upregulated in comparison I (fold change of 4.1) (**Figure 2**). The neurotransmitter *NPY* had the highest fold change in comparison II (fold change of 5.9) (**Figure 2**). Expression was highest in control tissue and PL-NAWM of chronic active MS lesions, lower in the rim of chronic active MS lesions, and lowest in inactive MS lesions (data not shown). The cytoplasmic protein *KANK4* had the highest *p*-value and was downregulated in the PL-NAWM of chronic active MS lesions compared to the PL-NAWM inactive lesions (comparison II; fold change of 0.3) (**Figure 2**). Expression was highest in inactive MS lesions and lower in control tissue and in chronic active MS lesions (data not shown). Finally, *NCAN* (neurocan), *TKTL1* (transketolase-like 1), and *ANO4* (anoctamin 4) were included because these were the only genes in cluster 3, with a specific peak in expression in the PL-NAWM of chronic active MS lesions (**Figure 3**). *NCAN* and *ANO4* are also upregulated in the PL-NAWM of chronic active MS lesions compared to the PL-NAWM of inactive lesions (comparison II; fold change of 2.7 and 2.1) (**Figure 2**). Immunohistochemical staining showed more explicit *ANO4* expression in the PL-NAWM of chronic active lesion compared to PL-NAWM of inactive MS lesion (**Figure S2** in Supplementary Material).

Validation and further characterization of genes of interest

There was a significant difference of the RIN value of control tissue compared to all MS lesion subareas, which is not unexpected as the control tissue was dissected in the cryostat using a scalpel as

opposed to laser-based microdissection of the MS tissue. This significant difference did not influence our conclusions, as microarray data were validated by qPCR (**Table 2**), which showed no effect of RIN value on expression levels when normalizing with housekeeping genes[20]. There was no significant difference in RIN values between the different MS lesion areas.

Table 2 | Selected genes of interest

	Comparison I chronic active rim vs inactive rim				Comparison II chronic active PL-NAWM vs inactive PL-NAWM				Comparison III chronic active PL-NAWM vs control			
	Microarray		**qPCR**		**Microarray**		**qPCR**		**Microarray**		**qPCR**	
Gene symbol	*p*-value	Fold change	*p*-value	Fold change	*p*-value	Fold change	*p*-value	Fold change	*p*-value	Fold change	*p*-value	Fold change
CHIT1	1.07E-18	10.2	7.00E-03	36.0	4.28E-02	2.0	n.d.	n.d.	n.s.	n.a.	1.20E-03	5.8
GPNMB	3.61E-08	8.0	3.00E-04	12.4	n.s.	n.a.	2.20E-03	8.3	7.40E-06	7.1	3.10E-03	6.7
CCL18	2.13E-15	6.8	4.76E-02	66.7	n.s.	n.a.	n.s.	n.a.	n.s.	n.a.	n.s.	n.a.
OLR1	2.76E-04	2.9	5.90E-03	3.2	4.36E-02	2.1	6.00E-04	7.5	4.86E-06	4.2	2.00E-04	6.0
CD68	1.55E-07	2.8	6.00E-04	5.2	3.15E-02	1.7	3.00E-04	4.8	3.16E-02	2.2	4.00E-04	5.0
MSR1	2.09E-04	2.8	5.90E-03	4.0	4.18E-02	1.8	2.05E-02	5.3	1.64E-04	4.8	7.00E-04	7.3
CXCL16	4.99E-04	1.8	1.75E-02	2.9	n.s.	n.a.	9.30E-03	2.8	n.s.	n.a.	n.s.	n.a.
CXCR4	1.08E-04	4.1	n.s.	n.a.	n.s.	n.a.	n.s.	n.a.	n.s.	n.a.	n.s.	n.a.
NPY	n.s.	n.a.	4.01E-02	6.0	1.15E-03	5.9	4.10E-03	22.9	n.s.	n.a.	n.s.	n.a.
KANK4	7.36E-09	0.4	1.40E-02	0.2	5.65E-06	0.3	n.s.	n.a.	n.s.	n.a.	6.80E-03	0.2

n.a. = not applicable; n.d. = not determined; n.s. = not significant; PL-NAWM = peri-lesional normal appearing white matter; qPCR = quantitative polymerase chain reaction.

Significant differences in gene expression were confirmed for *CHIT1, GPNMB, CCL18, KANK4, OLR1, CD68, MSR1,* and *CXCL16* in comparison I; for *NPY, OLR1, CD68*, and *MSR1* in comparison II; and for *GPNMB*, *OLR1*, *CD68*, and *MSR1* in comparison III. Some genes that showed no significant difference with microarray, did show a significant different with qPCR, e.g., *NPY* in comparison I, *GPNMB* and *CXCL16* in comparison II, and *CHIT1* and *KANK4* in comparison III. *CXCR4* showed no significant difference when validated with qPCR. The expression pattern for most genes was similar with qPCR as compared to the microarray. *CHIT1, GPNMB, CCL18, CXCR4, OLR1, CD68, MSR1,* and *CXCL16* all showed highest expression in the rim of chronic active MS lesions. *GPNMB, OLR1, CD68,* and *MSR1* were upregulated in comparison II and III, and *CXCL16* in comparison II. Expression of *NPY* was highest in control tissue and the PL-NAWM of chronic active MS lesions, lower in the rim of chronic active MS lesions, and lowest in inactive MS lesions. The expression pattern for *KANK4* was different with qPCR. Expression levels for *KANK4* peaked in inactive MS lesions with microarray, but showed a peak in control tissue with qPCR. Within MS subregions, *KANK4* expression was still highest in the rim of inactive MS lesions. Expression of CHIT1, GPNMB, and OLR1 was further investigated at the protein level by immunohistochemistry (**Figure 4**). CHIT1, GPNMB, and OLR1 were not detected in control tissue, but were clearly present in chronic active MS lesions in the gliotic center, the rim, and also the peri-rim, following the RNA expression pattern.

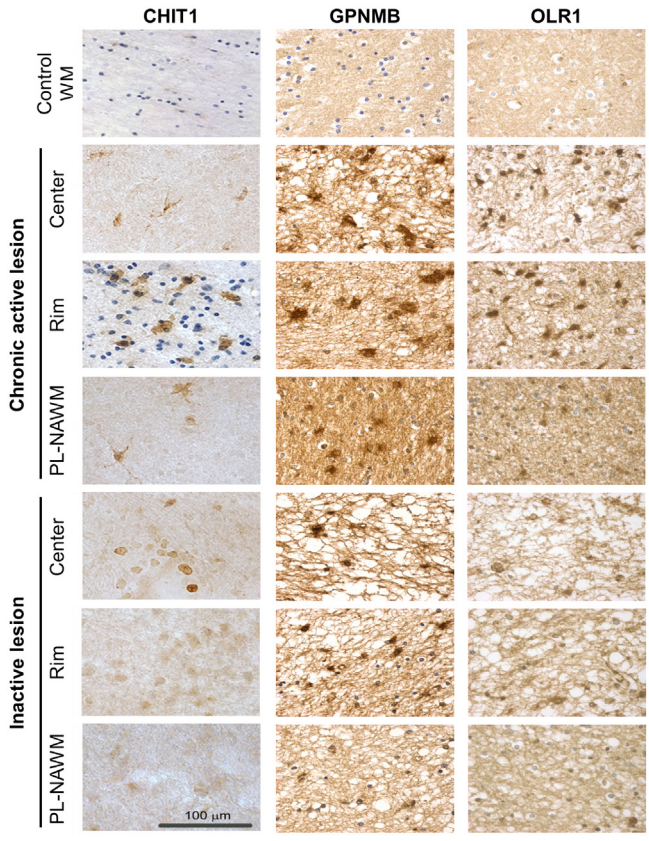

Figure 4 | Expression of CHIT1, GPNMB, and OLR1 in and around multiple sclerosis (MS) lesions. Protein expression of CHIT1, GPNMB, and OLR1 in control tissue and in the center, rim, and peri-lesional (PL)-normal appearing white matter (NAWM) of chronic active and inactive MS lesions determined by immunohistochemistry. Scale bar= 100 µm

In inactive MS lesions, only GPNMB expression was identified in the center of the lesion and the lesion rim. Protein expression of CD68, MSR1, and CXCL16 in and around chronic active MS lesions has been described previously by us[14]. Notably, these three genes have also been linked with Gaucher disease, a lysosomal storage disorder (see Discussion) and may relate to the process of myelin ingestion by microglia/macrophages. We next tested whether expression of CHIT1 and GPNMB is increased upon myelin uptake, as this has been demonstrated for CCL18[21]. Differentiated THP-1 macrophages were exposed to myelin from MS or control donors for 5 days, followed by 3 days culture in normal medium (**Figure 5**). After 8 days in culture, cells cultured with MS myelin showed a significant increase in *CHIT1* expression (p=0.02) and a trend toward more *GPNMB* (p=0.07) expression, compared to no myelin uptake. Uptake of myelin from control donors and myelin ingestion over time did not show an altered expression pattern. To conclude, both *CHIT1* and *GPNMB* are highly expressed in the rim and peri-rim of chronic active lesions, likely due to the uptake of MS myelin by microglia/macrophages.

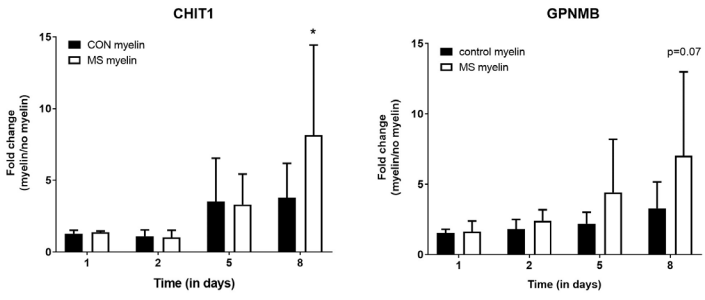

Figure 5 | Upregulation of *CHIT1* after uptake of multiple sclerosis (MS) myelin *in vitro*. At the mRNA level, both *CHIT1* (p=0.02) and *GPNMB* (p=0.007) are upregulated in THP-1 macrophages after incubation with myelin from MS donors for 5 days, followed by 3 days incubation in normal medium. Fold change from macrophages cultured without myelin, n=3, *$p < 0.05$.

The effect of scavenger receptor knockdown on myelin phagocytosis in vitro

As this study and our earlier work[14] revealed high expression of scavenger receptors in the rim as well as around chronic active MS lesions, we studied the role of OLR1, CD68, MSR1, and CXCL16 in an *in vitro* myelin phagocytosis assay (**Figure 6**). Antisense oligonucleotides were developed that downregulate expression of these genes in the human macrophage cell line THP-1, confirmed by qPCR (**Figure 6A**). Immunocytochemistry confirmed the efficient knockdown of MSR1 (**Figure 6B**). Knockdown of MSR1 and CXCL16 significantly decreased the percentage of macrophages that phagocytosed myelin and the total myelin phagocytosed, compared to untreated cells (**Figure 6C**). Phagocytosis of myelin derived from control or MS tissue was similarly reduced by MSR1 knockdown (**Figure 6D**).

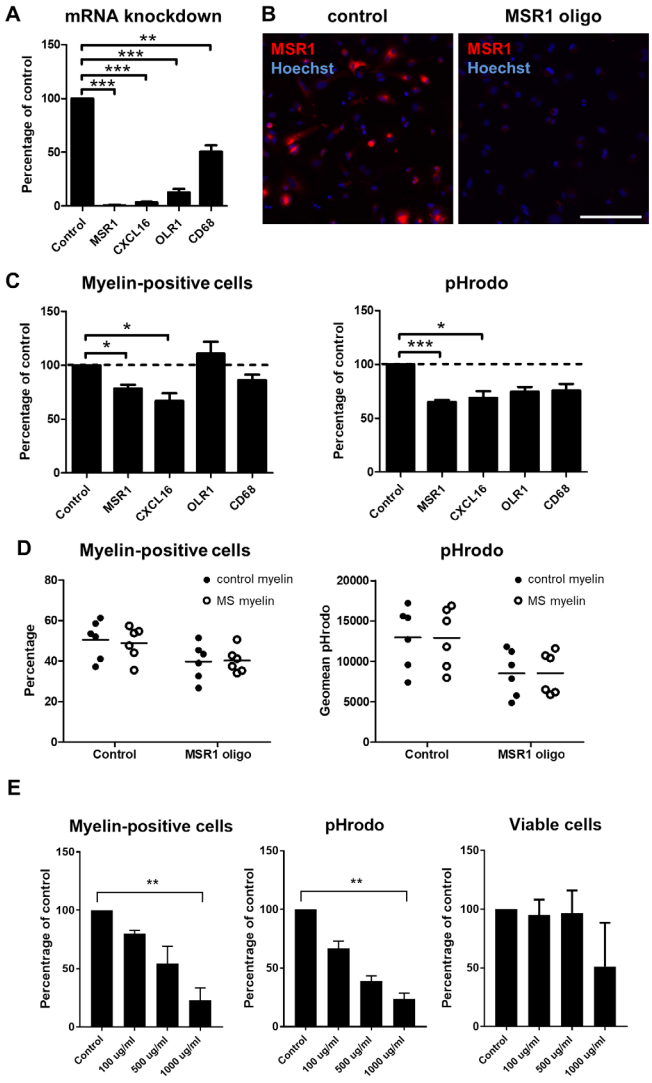

Figure 6 | Functional role of scavenger receptors in myelin phagocytosis *in vitro*. *MSR1, CXCL16, OLR1,* and *CD68* were downregulated with antisense oligonucleotides in the human macrophage cell line THP-1. Silencing efficiency was determined on mRNA level with quantitative polymerase chain reaction **(A)** and on protein level with immunocytochemistry [**(B)**; only shown for MSR1]. Uptake of pHrodo-labeled myelin was validated by flow cytometry **(C)** and compared for myelin obtained from control and multiple sclerosis (MS) brain tissue **(D)**. The number of cells that had phagocytosed myelin, and the total amount of myelin phagocytosed (geomean pHrodo) were calculated. The number of independent experiments (n) was 6 (MSR1), 4 (CXCL16), 3 (OLR1), and 3 (CD68). **E)** Fucoidan was used to inhibit a broad spectrum of scavenger receptors in THP-1 cells. Provided is the number of cells that had phagocytosed myelin, the total amount of myelin phagocytosed (geomean pHrodo), and the viability of cells at the time point of analysis (n=3). Scale bar in panel **(B)** = 200 μm $*p < 0.05$, $**p < 0.01$, $***p < 0.005$.

To block scavenger receptor function in a redundant manner, we also applied a broad pharmacological inhibitor[22,23]. Fucoidan showed a non-toxic, dose-dependent significant reduction of the percentage of macrophages that phagocytosed myelin and the total amount of myelin phagocytosed at 1,000 μg/ml (p=0.007; **Figure 6E**). Upregulation of scavenger receptors in chronic active MS lesions thus likely contributes to demyelination.

Discussion

In this study, we compared gene expression in and around chronic active MS lesions, inactive MS lesions, and control tissue to identify gene expression related to lesion activity and lesion halt. We found upregulation of genes involved in immune function, lipid binding, and lipid uptake in the active rim. This confirms the expectation, since in rims of chronic active lesions, inflammatory microglia/macrophage phagocytose myelin. Importantly, around chronic active MS lesions, genes involved in lipid binding and uptake also showed increased expression. This indicates early demyelination around chronic active lesions, showing that these lesions are indeed expanding. In addition, genes with a possible anti-inflammatory and/or neuroprotective function were upregulated in rims and around chronic active expanding lesions, possibly relating to the induction of endogenous protective mechanisms. Based on direct comparisons and cluster analysis, and with a specific focus on genes related to lesion activity and expansion, we identified several genes of interest: *CHIT1, GPNMB, CCL18, OLR1, CD68, MSR1, CXCL16, CXCR4, NPY, KANK4, NCAN, TKTL1,* and *ANO4*.

Altered gene expression in the rim and PL-NAWM of chronic active and inactive MS lesions

To visualize gene expression during MS lesion progression, we used the set-up as shown in Figure 1, which was thought to best resemble the sequence of events in MS lesion formation and progression. Cluster analysis (Figure 3) revealed six different expression patterns representing overall differences between control and MS (clusters 1 and 2), specific upregulation only around expanding, chronic active lesions (cluster 3), specific upregulation in active rims (cluster 4), upregulation in active rims and around inactive lesions, but low activity around active rims (cluster 5), or upregulation in and around inactive lesions, but low activity in active rims (cluster 6). Overrepresented genes within each cluster were detected by GO analysis (Table S4 in Supplementary Material). Clusters 2 and 4 showed genes involved in immune functions, which is expected as these genes peak in the rim of chronic active MS lesions. Not unexpected, genes involved in the lysosomal activity were overrepresented in cluster 4, corresponding with the process of demyelination. Genes involved in sterol and steroid metabolism were overrepresented in cluster 6, possibly indicating an attempt to repair damaged axons and myelin after active demyelination has diminished. In cluster 3, only three genes were regulated (discussed below).

The GO analysis also showed a shift in the expression location of overrepresented genes from the plasma membrane to the lysosomal membrane from comparison II to comparison I (data not shown). This is not surprising, as myelin first needs to be recognized and phagocytosed, before it can

be processed in the lysosomes. Furthermore, processes involved in lipid metabolism were overrepresented in comparison I (data not shown), indicating that phagocytosed myelin is being processed.

Joint upregulation of CHIT1, GPNMB, and CCL18 is mediated by myelin uptake

Our study identified *CHIT1, GPNMB*, and *CCL18* as top-3 upregulated genes in the rim of chronic active MS lesions, where foamy, myelin-accumulating microglia/macrophages are abundant. Interestingly, also in regions surrounding chronic active lesions, *CHIT1* and *GPNMB* were upregulated. Enhanced expression of *CCL18* in myelin-laden macrophages *in vitro* and in the rim and center of active MS lesions has been reported before[21]. Here, we demonstrate a relation between the regulation of both, *CHIT1* and *GPNMB*, and myelin uptake. Both genes showed an increased expression in THP-1-derived macrophages after 8 days of incubation with MS myelin, and not with control myelin, suggesting that specifically myelin derived from MS donors induce *CHIT1* and *GPNMB* expression. Wheeler and colleagues already reported that the composition of MS myelin in NAWM is altered, compared to control myelin[24], and previously, we described that MS myelin is taken up more efficiently[18].

Of note, upregulation of *CHIT1* and *CCL18* in lipid-laden macrophages of Gaucher patients has long been known[25,26]. More recently, CHIT1 has been described as a prognostic biomarker for early MS[27,28], and soluble GPNMB, which is secreted from different cell types through a disintegrin and metalloproteinase 10 sheddase activity, was identified as a further biomarker of Gaucher disease[29,30]. Co-regulation of *CHIT1, GPNMB,* and *CCL18* strengthens the idea that lipid-accumulating Gaucher cells and myelin-phagocytosing microglia/macrophages share cellular characteristics[21], possibly related to lysosomal stress, a function overrepresented in active rims (cluster 4). The precise relationship between the induction of CHIT1, GPNMB, and CCL18, myelin processing, and lysosomal activities of microglia in MS warrants further investigation.

Functional studies have linked CHIT1, GPNMB, and CCL18 primarily with the suppression of inflammation. Inhibition of CHIT1 in a mouse macrophage cell line induced a pro-inflammatory phenotype *in vitro*, caused downregulation of MSR1 and CD68, and decreased cholesterol uptake[31]. Notably, CHIT1 levels in the CSF reliably indicate microglial activation in clinical trials[32]. GPNMB was upregulated in astrocytes and neurons in an animal model of amyotrophic lateral sclerosis, and secretion of the extracellular fragment by astrocytes had a neuroprotective effect[33]. Another study showed that GPNMB was mainly expressed by macrophages/microglia in the rat brain and was upregulated in inflammatory conditions[34], acting as a negative regulator to prevent excessive immune responses[35]. In line herewith, Gpnmb-deficient mice (DC-HIL$^{-/-}$) manifested exacerbated autoimmune encephalomyelitis (EAE)[36]. Finally, CCL18 recruited a subset of human regulatory T cells *in vitro*, which suppressed proliferation of effector T cells via interleukin-10 production[37]. CCL18 is also produced by macrophages that have ingested myelin and show an immunosuppressive phenotype[21]. Suppressive effects on inflammation by CHIT1, GPNMB, and CXCL18 in relation to demyelination in regions surrounding active MS lesions need to be elucidated.

Scavenger receptors upregulated in and around chronic active MS lesions mediate myelin uptake

Myelin uptake during demyelination likely depends on scavenger receptors. We found *OLR1, CD68, MSR1,* and *CXCL16* upregulated in all three comparisons (*CXCL16* only in comparison I and in comparison II with qPCR). Thus, these scavenger receptors are upregulated in chronic active rims, but also around chronic active lesions, indicating that they are involved in early demyelination. We cannot fully exclude some contamination of PL regions with rim tissue during laser dissection, but early demyelination around chronic active lesions is further indicated by immunohistochemistry, showing upregulation of CHIT1, GPNMB, and OLR1 in and around chronic active MS lesions. These results extends our earlier work, showing enhanced expression of *CD68, MSR1*, and *CXCL16* in and around chronic active MS lesions, compared to control tissue[14]. CD68 is a scavenger receptor predominantly expressed on the lysosomal membrane, but the small percentage expressed on the plasma membrane is capable of oxLDL phagocytosis[38,39]. SA-RI/II, encoded by MSR1, was shown to be directly involved in myelin uptake *in vitro*[40–42], and Msr1$^{-/-}$ mice showed less severe disease and reduced demyelination in the EAE model[43]. CXCL16 has a dual function as a scavenger receptor and as a chemokine in soluble form. Neutralizing antibodies against CXCL16 delayed the onset and reduced the severity of EAE in mice[44]. The soluble form is elevated in MS patients, compared to control subjects[45]. This indicates that scavenger receptors could be actively involved in demyelination in MS. Furthermore, their upregulation in the PL-NAWM of chronic active MS lesions, might suggest they are involved in the initial stages of MS lesion development and progression.

The functional role of OLR1, CD68, MSR1, and CXCL16 was studied in an *in vitro* myelin phagocytosis assay, using the human macrophage cell line THP-1. All genes were significantly downregulated, compared to untreated cells. Downregulation of MSR1 and CXCL16 resulted in a significant decrease in the number of myelin-phagocytosing cells and total myelin uptake. A direct role of MSR1 in myelin phagocytosis in MS is consistent with earlier research[40–42] and supported by its expression in regions of active demyelination in MS brain tissue. Its upregulation in the PL-NAWM of chronic active MS lesions could indicate that phagocytosing cells in yet unaffected areas are already preparing for demyelination. Notably, pharmacological inhibition of a broad spectrum of scavenger receptors by fucoidan further reduced the number of phagocytosing macrophages and the total amount of myelin uptake, indicating that a combination of scavenger receptors contributes to the uptake of myelin.

Molecules associated with lesion expansion

Our analysis identified many more genes regulated in and around chronic active and inactive MS lesions, which are potential targets to regulate lesion expansion. *NCAN, TKTL1*, and *ANO4* were of specific interest because they peaked at the PL-NAWM of chronic active MS lesions (cluster 3). Consistent with our findings, an upregulation of the extracellular matrix component NCAN in the rim and also slightly in the PL-NAWM of MS lesions has been reported earlier[46]. Furthermore, NCAN is expressed by astrocytes and known to be upregulated after brain injury and modulates neuronal outgrowth[47]. TKTL1 is a transketolase expressed by mature oligodendrocytes in PL-NAWM of MS

lesions and by oligodendrocyte precursors, reactive astrocytes, and macrophages in the rim of MS lesions[48] that has been postulated to prevent neurodegeneration by reducing the formation of advanced glycation end products and radicals[49]. Upregulation of *TKTL1* might be an initial protective reaction to changes taking place in the PL-NAWM of MS lesions. Both *NCAN* and *TKTL1* might be important regulators in early axonal damage. Finally, the potential role of *ANO4*, a suggested Ca^{2+}-dependent lipid scramblase, in MS lesion development is unknown. In contrast to chronic active lesions, the PL-NAWM of inactive lesions show overrepresented genes involved in sterol biosynthesis, which might indicate an attempt to restore damaged tissue and myelin after active demyelination has diminished.

Both *KANK4* and *NPY* are regulated in the RIM and PL-NAWM of chronic active lesion, where *KANK4* was downregulated and *NPY* showed an upregulation. KANK family proteins are involved in the inhibition of actin stress fibers formation and cell motility [reviewed in Ref.[50]], but the exact function of KANK4 and its role in MS lesions formation needs to be determined. In contrast to *KANK4*, the neurotransmitter *NPY* was upregulated in chronic active lesions. Application of NPY during EAE induction significantly suppressed clinical signs in DA rats[51] and in mice[52]. NPY also inhibited disease and reduced inflammation when administered after the onset of EAE symptoms[53]. Fc receptor-dependent phagocytosis of opsonized latex beads by lipopolysaccharide-stimulated microglia was reduced by NPY[54]. Induction of NPY in and around acute MS lesions, might regulate myelin phagocytosis and immune suppression during early demyelination events.

Studying gene expression profiles associated with expansion of chronic active MS lesions is essential, since we recently showed that chronic active lesions highly correlate to disease progression (Luchetti *et al.*, submitted). Taken together, we found changes in immune activation and lipid uptake in the rim of chronic active MS lesions. Genes related to lipid phagocytosis were also upregulated in the PL-NAWM of chronic active MS lesions, showing that chronic active lesions indeed expand. Importantly, potentially protective, anti-inflammatory genes were also upregulated in the (peri)-rim of chronic active MS lesions, suggesting a vain attempt to prevent lesion expansion and progression. We functionally confirmed the ability of the scavenger receptors MSR1 and CXCL16 to mediate myelin uptake. Our results pinpoint scavenger receptors as interesting targets to stop demyelination around chronic active lesions, which could block lesion expansion.

Acknowledgements

The authors acknowledge the Netherlands Brain Bank (http://www.brainbank.nl) for providing the donor material, Dr. Marie Orre and Dr. Matthew Mason for help with the data analysis, and Katerina Konstantoulea for experimental help. DH and MP were financially supported by the Dutch MS Research Foundation (grants MS 08-659 and MS 13-830).

Data availability

Microarray data have been uploaded in the Gene Expression Omnibus (GEO) database. The GEO accession number to access the complete dataset is: GSE108000.

References

1. Ascherio, A., Munger, K. L. & Lünemann, J. D. The initiation and prevention of multiple sclerosis. *Nat. Rev. Neurol.* **8**, 602–612 (2012).

2. Hedstrom, A. K., Alfredsson, L. & Olsson, T. Environmental factors and their interactions with risk genotypes in MS susceptibility. *Curr. Opin. Neurol.* **29**, 293–298 (2016).

3. van Der Valk, P. & De Groot, C. J. A. Staging of multiple sclerosis (MS) lesions: Pathology of the time frame of MS. Neuropathol. *Appl. Neurobiol.* **26**, 2–10 (2000).

4. Kuhlmann, T. *et al.* An updated histological classification system for multiple sclerosis lesions. *Acta Neuropathol.* **133**, 13–24 (2017).

5. Dal, A. *et al.* Slow expansion of multiple sclerosis iron rim lesions: pathology and 7 T magnetic resonance imaging. *Acta Neuropathol.* **133**, 25–42 (2017).

6. Lindberg, R. L. P. *et al.* Multiple sclerosis as a generalized CNS disease — comparative microarray analysis of normal appearing white matter and lesions in secondary progressive MS. *J. Neurochem.* **152**, 154–167 (2004).

7. Mycko, M. P., Papoian, R., Boschert, U., Raine, C. S. & Selmaj, K. W. cDNA microarray analysis in multiple sclerosis lesions: Detection of genes associated with disease activity. *Brain* **126**, 1048–1057 (2003).

8. Mycko, M. P., Papoian, R., Boschert, U., Raine, C. S. & Selmaj, K. W. Microarray gene expression profiling of chronic active and inactive lesions in multiple sclerosis. *Clin. Neurol. Neurosurg.* **106**, 223–229 (2004).

9. Tajouri, L. *et al.* Quantitative and qualitative changes in gene expression patterns characterize the activity of plaques in multiple sclerosis. *Mol. Brain Res.* **119**, 170–183 (2003).

10. Whitney, L. W., Ludwin, S. K., McFarland, H. F. & Biddison, W. E. Microarray analysis of gene expression in multiple sclerosis and EAE identifies 5-lipoxygenase as a component of inflammatory lesions. *J. Neuroimmunol.* **121**, 40–48 (2001).

11. Fischer, M. T. *et al.* NADPH oxidase expression in active multiple sclerosis lesions in relation to oxidative tissue damage and mitochondrial injury. *Brain* **135**, 886–899 (2012).

12. Zeis, T., Graumann, U., Reynolds, R. & Schaeren-Wiemers, N. Normal-appearing white matter in multiple sclerosis is in a subtle balance between inflammation and neuroprotection. *Brain* **131**, 288–303 (2008).

13. Koning, N., Bo, L., Hoek, R. M. & Huitinga, I. Downregulation of Macrophage Inhibitory Molecules in Multiple Sclerosis Lesions. *Ann. Neurol.* **62**, 504–514 (2007).

14. Hendrickx, D. A. E. *et al.* Selective upregulation of scavenger receptors in and around demyelinating areas in multiple sclerosis. *J. Neuropathol. Exp. Neurol.* **72**, 106–18 (2013).

15. Sharov, A. A., Dudekula, D. B. & Ko, M. S. H. A web-based tool for principal component and significance analysis of microarray data. *Bioinformatics* **21**, 2548–2549 (2005).

16. Livak, K. J. & Schmittgen, T. D. Analysis of relative gene expression data using real-time quantitative PCR and the 2(-Delta Delta C(T)) Method. *Methods* **25**, 402–408 (2001).

17. Stein, C. A. *et al.* Efficient gene silencing by delivery of locked nucleic acid antisense oligonucleotides, unassisted by transfection reagents. Nucleic Acids Res. 38, e3 (2010).

18. Hendrickx, D. A. E., Schuurman, K. G., van Draanen, M., Hamann, J. & Huitinga, I. Enhanced uptake of multiple sclerosis-derived myelin by THP-1 macrophages and primary human microglia. *J. Neuroinflammation* **11**, 64 (2014).

19. Beißbarth, T. & Speed, T. P. GOstat: Find statistically overrepresented Gene Ontologies with a group of genes. *Bioinformatics* **20**, 1464–1465 (2004).

20. Fleige, S. & Pfaffl, M. W. RNA integrity and the effect on the real-time qRT-PCR performance. *Mol. Cell. Proteomics* **27**, 126–139 (2006).

21. Boven, L. A. *et al.* Myelin-laden macrophages are anti-inflammatory, consistent with foam cells in multiple sclerosis. *Brain* **129**, 517–526 (2006).

22. Krieger, M. & Herz, J. Structures and fucntions of receptors: Macrophage Scavenger Receptors and LDL receptor-related protein (LRP). *Annu. Rev. Biochem.* **63**, 601–37 (1994).

23. Wang, R., Ph, D. & Chandawarkar, R. Y. Phagocytosis of Fungal Agents and Yeast Via Macrophage Cell Surface Scavenger Receptors. *J. Surg. Res.* **164**, e273–e279 (2010).

24. Wheeler, D., Bandaru, V. V. R., Calabresi, P. A., Nath, A. & Haughey, N. J. A defect of sphingolipid metabolism modifies the properties of normal appearing white matter in multiple sclerosis. *Brain* **131**, 3092–3102 (2008).

25. Boot, R. G. *et al.* Marked elevation of the chemokine CCL18/PARC in Gaucher disease: a novel surrogate marker for assessing therapeutic intervention. *Blood* **103**, 33–40 (2004).

26. Boven, L. A. *et al.* Gaucher cells demonstrate a distinct macrophage phenotype and resemble alternatively activated macrophages. *Am. J. Clin. Pathol.* **122**, 359–369 (2004).

27. Møllgaard, M., Degn, M., Sellebjerg, F., Frederiksen, J. L. & Modvig, S. Cerebrospinal fluid chitinase-3-like 2 and chitotriosidase are potential prognostic biomarkers in early multiple sclerosis. *Eur. J. Neurol.* **23**, 898–905 (2016).

28. Novakova, L. *et al.* Cerebrospinal fluid biomarkers as a measure of disaese activity and treatment efficacy in relapsing-remitting multiple sclerosis. *J. Neurochem.* **141**, 296–304 (2017).

29. Kramer, G. *et al.* Elevation of glycoprotein nonmetastatic melanoma protein B in type 1 Gaucher disease patients and mouse models. *FEBS Open Bio* **6**, 902–913 (2016).

30. Murugesan, V. *et al.* Validating glycoprotein non-metastatic melanoma B (gpNMB, osteoactivin), a new biomarker of Gaucher disease. *Blood Cells, Mol. Dis.* **68**, 47–53 (2016).

31. Kitamoto, S. *et al.* Chitinase inhibition promotes atherosclerosis in hyperlipidemic mice. *Am. J. Pathol.* **183**, 313–325 (2013).

32. Olsson, B., Malmestr, C., Andreasen, N., Zetterberg, H. & Blennow, K. Extreme Stability of Chitotriosidase in Cerebrospinal Fluid makes it a Suitable Marker for Microglial Activation in Clinical Trials. *J. Alzheimer's Dis.* **32**, 273–276 (2012).

33. Tanaka, H. *et al.* The potential of GPNMB as novel neuroprotective factor in amyotrophic lateral sclerosis. *Sci. Rep.* **2**, 573 (2012).

34. Huang, J-J., Ma, W-J. & Yokoyama, S. Expression and immunolocalization of Gpnmb, a glioma-associated glycoprotein, in normal and inflamed central nervous systems of adult rats. *Brain Behav.* **2**, 85–96 (2012).

35. Ripoll, V. M. *et al.* Gpnmb Is Induced in Macrophages by IFN-γ and Lipopolysaccharide and Acts as a Feedback Regulator of Proinflammatory Responses. *J. Immunol.* **178**, 6557–6566 (2015).

36. Chung, J.S., Tamura, K., Akiyoshi, H., Cruz, P. D. & Ariizumi, K. The DC-HIL/Syndecan-4 Pathway Regulates Autoimmune Responses through Myeloid-Derived Suppressor Cells. *J. Immunol.* **192**, 2576–2584 (2014).

37. Chenivesse, C. et al. Pulmonary CCL18 Recruits Human Regulatory T Cells. *J. Immunol.* **189**, 128–137 (2012).

38. Ramprasad, M. P., Terpstra, V., Kondratenko, N., Quehenberger, O. & Steinberg, D. Cell surface expression of mouse macrosialin and human CD68 and their role as macrophage receptors for oxidized low density lipoprotein. *Proc. Natl. Acad. Sci.* **93**, 14833–14838 (1996).

39. Kurushima, H. *et al.* Surface expression and rapid internalization of macrosialin (mouse CD68) on elicited mouse peritoneal macrophages. *J. Leukoc. Biol.* **67**, 104–8 (2000).

40. Da Costa, C., van Der Laan, L. J. W., Dijkstra, C. D. & Brück, W. The role of the mouse macrophage scavenger receptor in myelin phagocytosis. *Eur. J. Neurosci.* **9**, 2650–2657 (1997).

41. Reichert, F. & Rotshenker, S. Complement-receptor-3 and scavenger-receptor-AI/II mediated myelin phagocytosis in microglia and macrophages. *Neurobiol. Dis.* **12**, 65–72 (2003).

42. Wållberg, M., Bergquist, J., Achour, A., Breij, E. & Harris, R. A. Malondialdehyde modification of myelin oligodendrocyte glycoprotein leads to increased immunogenicity and encephalitogenicity. *Eur. J. Immunol.* **37**, 1986–1995 (2007).

43. Levy-Barazany, H. & Frenkel, D. Expression of Scavenger receptor A on antigen presenting cells is important for CD4+ T-cells proliferation in EAE mouse model. *J. Neuroin.* **9**, 120 (2012).

44. Fukumoto, N. *et al.* Critical Roles of CXC Chemokine Ligand 16/Scavenger Receptor that Binds Phosphatidylserine and Oxidized Lipoprotein in the Pathogenesis of Both Acute and Adoptive Transfer Experimental Autoimmune Encephalomyelitis. *J. Immunol.* **173**, 1620–1627 (2004).

45. Le Blanc, L. M. P. *et al.* CXCL16 is elevated in the cerebrospinal fluid versus serum and in inflammatory conditions with suspected and proved central nervous system involvement. *Neurosci. Lett.* **397**, 145–148 (2006).

46. Sobel, R. A. & Ahmed, A. S. White matter extracellular matrix chondroitin sulfate/dermatan sulfate proteoglycans in multiple sclerosis. *J. Neuropathol. Exp. Neurol.* **60**, 1198–1207 (2001).

47. Tang, X., Davies, J. E. & Davies, S. J. A. Changes in Distribution, Cell Associations, and Protein Expression Levels of NG2, V2, and Tenascin-C During Acute to Chronic Maturation of Spinal Cord Scar Tissue. *J. Neurosci. Res.* **71**, 427–444 (2003).

48. Lovato, L. *et al.* Transketolase and 2',3'-Cyclic-nucleotide 3'-Phosphodiesterase Type I Isoforms Are Specifically Recognized by IgG Autoantibodies in Multiple Sclerosis Patients. *Mol. Cell. Proteomics* **7**, 2337–2349 (2008).

49. Coy, J. F., Dressler, D., Wilde, J. & Schubert, P. Mutations in the transketolase-like gene TKTL1: clinical implications for neurodegenerative diseases, diabetes and cancer. *Clin. Lab.* **51**, 257–273 (2005).

50. Kakinuma, N., Roy, B. C., Zhu, Y., Wang, Y. & Kiyama, R. Kank regulates RhoA-dependent formation of actin stress fibers and cell migration via 14-3-3 in PI3K-Akt signaling. *J. Cell Biol.* **181**, 537–549 (2008).

51. Dimitrijevi, M., Miti, K., Vuji, V. & Stanojevi, S. NPY suppressed development of experimental autoimmune encephalomyelitis in Dark Agouti rats by disrupting costimulatory molecule interactions. *J. Immunol.* **245**, 23–31 (2012).

52. Bedoui, S. *et al.* Neuropeptide Y (NPY) Suppresses Experimental Autoimmune Encephalomyelitis: NPY1 Receptor-Specific Inhibition of Autoreactive Th1 Responses In Vivo. *J. Immunol.* **171**, 3451–3458 (2003).

53. Brod, S. A. & Bauer, V. L. Ingested (oral) neuropeptide Y inhibits EAE. *J. Neuroimmunol.* **250**, 44–49 (2012).

54. Ferreira, R. *et al.* Neuropeptide Y inhibits interleukin-1b-induced phagocytosis by microglial cells. *J. Neuroinflammation* **8**, 1–15 (2011).

Supplemental Material

Supplemental Table 1 | Donor characteristics

NBB no.	Tissue	Age	Sex	Type	Duration	Cause of death	PMD	pH	IHC
1995-043	C	75	M			Sepsis, adenocarcinoma	07:20	6.16	
1996-014	C	54	F			Renal failure	08:00	6.45	
1996-032	C	60	F			Legal euthanasia	08:25	6.6	
1996-129	C	70	M			Pancreas carcinoma	07:30	6.4	
1997-042	C	65	F			Cardiac arrest	12:50	6.94	
2000-025	C	41	F			Bleeding from adenocarcinoma	13:30	6.23	
2000-050	C	52	F			Metastasized leiomyosarcoma	06:50	7.16	
2001-069	C	68	F			Legal euthanasia	07:37	5.45	+
2008-073	C	50	F			Metastasized broncho-carcinoma	04:10	6.98	
2009-003	C	62	M			U	07:20	6.36	+
1996-121	CA	53	F	RR	18	Pneumonia	07:16	6.54	
1997-160	CA	40	F	RR	11	Pneumonia	07:00	6.33	
1999-051	CA	45	F	RR	14	Legal euthanasia	10:55	6.62	+
2001-018	CA	48	F	RR	9	Legal euthanasia	08:10	6.55	
2001-135	CA	43	M	RR	17	Pneumonia	08:30	6.48	+
2007-085	CA	66	F	RR	23	U	06:00	6.18	+
2010-025	CA	51	M	SP	>20	U	11:00	6.23	+
2001-093	I	66	F	RR	43	Liver failure	06:20	6.44	
2002-023	I	75	F	RR	34	Pneumonia	08:00	6.5	
2002-063	I	72	F	RR	14	Pneumonia	12:00	6.85	+
2008-053	I	64	F	RR	39	Urosepsis	10:10	6.3	
2008-100	I	77	F	RR	24	Legal euthanasia	10:00	6.5	+
2009-034	I	45	M	RR	19	Pulmonary embolism	07:45	6.22	+
2009-047	I	50	M	PP	24	U	09:30	6.2	
2009-067	I	44	M	PP	13	Pneumonia	12:00	6.06	+
2010-040	I	57	F	U	25	Legal euthanasia	08:40	6.44	

Age = age at death (years); C = control subject; CA = chronic active MS; Duration = disease duration (years); F = female; I = inactive MS; IHC = immunohistochemistry; M = male; NBB no. = donor registration number of the Netherlands Brain Bank; pH = pH of CSF; PMD = post-mortem delay (h:min); PP = primary progressive MS; RR = relapsing-remitting MS; Tissue = tissue type; Type = clinical subtype of MS; U = unknown.

Supplemental Table 2 | Primer pairs used for qPCR

Gene symbol	Forward sequence (5′–3′)	Reverse sequence (5′–3′)

CHIT1	TGCGCAAATACAGCTTTGAC	ACCTCGTATCCAGCATCCAC
GPNMB	GCTGACTGTGAGACGAACCT	ACAGAAATCAGGGTGCTCGT
CCL18	CCCAGCTCACTCTGACCACT	GTGGAATCTGCCAGGAGGTA
CXCR4	TTCCCTCTAGTGGGCGGGG	AAAGGGCACTGAGACGCTGA
NPY	CATCACCAGGCAGAGATATGGA	ATCACCACATTGCAGGGTCT
KANK4	GCTCGCCAAGAACCTTCAAC	GGTCTTTCTCTTCATCCCCCT
NCAN	AGTCCCGTCCTGGTTGCTATG	ATCGTAGAGTTCCTGTGGGTTG
TKTL1	GCTCCGGCCACCCTACATC	GCCACATCCACAAACGACAG
ANO4	ATTTTGCCTGGTTGGGCTGG	ACTTCTTTACTGACTTGGCTGTG
MSR1	TTCAAAGCTGCACTGATTGCC	TTCTTCGTTTCCCACTTCAGGA
CD68	ACGCAGCACAGTGGACATTCT	TGATGCTCGAGTTGCTGCA
CXCL16	GCCATCGGTTCAGTTCATGA	AAAGGAGCTGGAACCTCGTGT
OLR1	TTACTCTCCATGGTGGTGCCT	TGCCCAGCACCATAATGGT
GAPDH	TGCACCACCAACTGCTTAGC	GGCATGGACTGTGGTCATGA
TUBA1A	CTTTGAGCCAGCCAACCAGA	GTACAACAGGCAGCAAGCCAT
EF1α	AAGCTGGAAGATGGCCCTAAA	AAGCGACCCAAAGGTGGAT

Supplemental Table 3A | Top 50 upregulated genes in chronic active rim vs inactive rim (comparison I)

Gene symbol	Gene name	Adjusted *p*-value	Fold change
CHIT1	chitinase 1 (chitotriosidase)	1.07E-18	10.2
GPNMB	glycoprotein (transmembrane) nmb, transcript variant 1	3.61E-08	8.0
CCL18	chemokine (C-C motif) ligand 18 (pulmonary and activation-regulated)	2.13E-15	6.8
ACP5	acid phosphatase 5, tartrate resistant, transcript variant 4	9.86E-15	6.4
PKD2L1	polycystic kidney disease 2-like 1	8.91E-18	5.7
HLA-DQA1	major histocompatibility complex, class II, DQ alpha 1	3.19E-04	4.7
FCGR2B	Fc fragment of IgG, low affinity IIb, receptor (CD32), transcript variant 1	8.81E-11	4.6
CFD	complement factor D (adipsin)	2.48E-07	4.5
APOC1	apolipoprotein C-I	9.12E-07	4.4
CXCR4	chemokine (C-X-C motif) receptor 4, transcript variant 1	1.08E-04	4.1
PLA2G7	phospholipase A2, group VII (platelet-activating factor acetylhydrolase, plasma)	4.86E-10	4.0
HS3ST2	heparan sulfate (glucosamine) 3-O-sulfotransferase 2	4.68E-08	4.0
IFI30	interferon, gamma-inducible protein 30	4.54E-08	3.6
CAPG	capping protein (actin filament), gelsolin-like	1.24E-06	3.2
RAB42	RAB42, member RAS oncogene family	2.56E-07	3.0
MS4A7	membrane-spanning 4-domains, subfamily A, member 7, transcript variant 1	1.02E-05	3.0
ITGAX	integrin, alpha X (complement component 3 receptor 4 subunit)	5.41E-05	2.9
AMICA1	adhesion molecule, interacts with CXADR antigen 1, transcript variant 2	2.89E-09	2.9
DENND2D	DENN/MADD domain containing 2D	5.11E-08	2.9
OLR1	oxidized low density lipoprotein (lectin-like) receptor 1	2.76E-04	2.9
ALOX5AP	arachidonate 5-lipoxygenase-activating protein	1.51E-05	2.8
FGR	Gardner-Rasheed feline sarcoma viral (v-fgr) oncogene homolog, transcript variant 2	1.34E-05	2.8
CD68	CD68 molecule, transcript variant 1	1.55E-07	2.8
IRF5	interferon regulatory factor 5, transcript variant 1	4.33E-03	2.8
MSR1	macrophage scavenger receptor 1 (MSR1), transcript variant SR-AI	2.17E-04	2.8
ASCL2	achaete-scute complex homolog 2 (Drosophila)	8.53E-08	2.8
HLA-DMB	major histocompatibility complex, class II, DM beta	1.43E-03	2.8
SLC7A7	solute carrier family 7 (cationic amino acid transporter, y+ system), member 7, transcript variant 1	1.54E-06	2.8
TNFAIP2	tumor necrosis factor, alpha-induced protein 2	1.30E-06	2.7
BCL2A1	BCL2-related protein A1, transcript variant 1	3.17E-04	2.7
HLA-DRB5	major histocompatibility complex, class II, DR beta 5	2.04E-02	2.7
ADORA3	adenosine A3 receptor, transcript variant 1	5.84E-06	2.7
SLC47A1	solute carrier family 47, member 1	1.60E-13	2.7
MX2	myxovirus (influenza virus) resistance 2 (mouse)	2.13E-11	2.7
S100A11	S100 calcium binding protein A11	2.14E-06	2.6
NCF2	neutrophil cytosolic factor 2, transcript variant 1	1.63E-05	2.6
CD83	CD83 molecule, transcript variant 1	8.82E-05	2.6
FCGR2C	Fc fragment of IgG, low affinity IIc, receptor for (CD32)	2.13E-06	2.6
ENST00000424686	Major histocompatibility complex, class II, DQ beta 1	2.83E-03	2.6
HLA-DQA2	major histocompatibility complex, class II, DQ alpha 2	1.28E-04	2.6
SIGLEC8	sialic acid binding Ig-like lectin 8	4.72E-06	2.6
ENST00000412049	HLA class II histocompatibility antigen, DQ(2) alpha chain Precursor	3.34E-03	2.6
CCRL2	chemokine (C-C motif) receptor-like 2, transcript variant 1	5.68E-08	2.5
MS4A4A	membrane-spanning 4-domains, subfamily A, member 4, transcript variant 1	7.22E-03	2.5

Supplemental Table 3A *(continued)*

Gene symbol	Gene name	Adjusted *p*-value	Fold change
FCER1G	Fc fragment of IgE, high affinity I, receptor for; gamma polypeptide	2.26E-06	2.5
HPSE	heparanase, transcript variant 1	2.04E-08	2.5
LAPTM5	lysosomal protein transmembrane 5	2.32E-03	2.5
LSP1	lymphocyte-specific protein 1, transcript variant 3	7.54E-03	2.5
HLA-DMA	major histocompatibility complex, class II, DM alpha	2.44E-04	2.5
KLHL6	kelch-like 6 (Drosophila)	8.32E-08	2.5

Supplemental Table 3B | Top 50 downregulated genes in chronic active rim vs inactive rim (comparison I)

Gene symbol	Gene name	Adjusted *p*-value	Fold change
HBB	hemoglobin, beta	1.44E-02	0.3
HBD	hemoglobin, delta	1.35E-02	0.3
CRLF1	cytokine receptor-like factor 1	2.86E-02	0.3
ABCA6	ATP-binding cassette, sub-family A (ABC1), member 6	1.20E-02	0.3
KANK4	KN motif and ankyrin repeat domains 4	4.88E-08	0.3
RNU2-2	RNA, U2 small nuclear 2, small nuclear RNA	1.30E-03	0.4
DHCR24	24-dehydrocholesterol reductase	1.93E-06	0.4
TSPAN8	tetraspanin 8	1.71E-05	0.4
ENST00000392423	titin isoform novex-3	4.30E-04	0.4
SQLE	squalene epoxidase	6.39E-06	0.5
ENST00000313339	Ankyrin repeat domain-containing protein 18A	3.75E-04	0.5
RBM11	RNA binding motif protein 11	6.49E-06	0.5
RNU1-5	RNA, U1 small nuclear 5, small nuclear RNA	1.15E-03	0.5
FSTL5	follistatin-like 5, transcript variant 1	2.35E-04	0.5
RMRP	RNA component of mitochondrial RNA processing endoribonuclease	5.46E-03	0.5
WIF1	WNT inhibitory factor 1 (WIF1)	3.37E-04	0.5
TTN	titin (TTN), transcript variant N2-A	4.19E-03	0.5
RELN	reelin, transcript variant 1	2.11E-03	0.5
LOC728449	Putative uncharacterized protein ENSP00000334090	8.82E-05	0.5
TNFRSF21	tumor necrosis factor receptor superfamily, member 21	8.82E-05	0.5
LOC100133402	hypothetical LOC100133402	6.36E-03	0.5
C21orf130	chromosome 21 open reading frame 130, non-coding RNA	4.18E-02	0.5
LOC100290344	FLJ44107 fis, clone TESTI4044296	3.57E-03	0.5
PDE11A	phosphodiesterase 11A, transcript variant 4	1.45E-04	0.5
SNORA28	small nucleolar RNA, H/ACA box 28, small nucleolar RNA	2.74E-03	0.5
ANKRD20B	ankyrin repeat domain 20B, non-coding RNA	1.71E-04	0.5
LDLR	low density lipoprotein receptor	1.06E-02	0.5
ALAS2	aminolevulinate, delta-, synthase 2, nuclear gene encoding mitochondrial protein, transcript variant 1	1.40E-02	0.5
KLK6	kallikrein-related peptidase 6, transcript variant B	1.97E-04	0.5
RAPGEF5	Rap guanine nucleotide exchange factor (GEF) 5	8.11E-05	0.5
MBP	myelin basic protein, transcript variant 7	6.71E-04	0.5
F5	coagulation factor V (proaccelerin, labile factor)	3.75E-04	0.5
HAPLN2	hyaluronan and proteoglycan link protein 2	1.09E-03	0.5
ABCA8	ATP-binding cassette, sub-family A (ABC1), member 8	1.68E-03	0.5
NIPAL4	NIPA-like domain containing 4	2.62E-04	0.5
CDKN1C	cyclin-dependent kinase inhibitor 1C (p57, Kip2), transcript variant 1	1.69E-05	0.5
GDF10	growth differentiation factor 10	4.17E-03	0.5
MOBP	myelin-associated oligodendrocyte basic protein	5.58E-03	0.5
HN1L	hematological and neurological expressed 1-like	1.76E-04	0.5
ENPP6	ectonucleotide pyrophosphatase/phosphodiesterase 6	5.81E-03	0.5
LOC283713	cDNA FLJ37663 fis, clone BRHIP2011120	3.80E-03	0.5
DPYSL5	dihydropyrimidinase-like 5	1.97E-04	0.5
INSIG1	insulin induced gene 1, transcript variant 1	1.83E-02	0.5
LOC100008587	5.8S ribosomal RNA (LOC100008587), ribosomal RNA	2.20E-02	0.6

Supplemental Table 3B *(continued)*

Gene symbol	Gene name	Adjusted *p*-value	Fold change
TMEM125	transmembrane protein 125	4.85E-02	0.6
TMEM144	transmembrane protein 144	6.17E-03	0.6
SPOCK3	sparc/osteonectin, cwcv and kazal-like domains proteoglycan (testican) 3, transcript variant 2	2.18E-03	0.6
RHBDL2	rhomboid, veinlet-like 2 (Drosophila)	1.10E-03	0.6
ERMN	ermin, ERM-like protein, transcript variant 2	1.26E-02	0.6
DMBT1	deleted in malignant brain tumors 1, transcript variant 2	4.18E-02	0.6

Supplemental Table 3C | Top 50 upregulated genes in chronic active PL-NAWM vs inactive PL-NAWM (comparison II)

Gene symbol	Gene name	Adjusted *p*-value	Fold change
NPY	neuropeptide Y	1.15E-03	5.9
GABRA1	gamma-aminobutyric acid (GABA) A receptor, alpha 1, transcript variant 3	5.86E-03	3.9
SYNPR	synaptoporin, transcript variant 2	3.09E-03	3.8
NPTX1	neuronal pentraxin I	4.78E-02	3.7
VSNL1	visinin-like 1	3.72E-02	3.7
OPALIN	oligodendrocytic myelin paranodal and inner loop protein, transcript variant 3	7.36E-04	3.6
SYN2	synapsin II, transcript variant IIb	3.75E-02	3.5
SNAP25	synaptosomal-associated protein, 25kDa, transcript variant 1	4.47E-02	3.4
CREG2	cellular repressor of E1A-stimulated genes 2	2.12E-03	3.3
GABRB2	gamma-aminobutyric acid (GABA) A receptor, beta 2, transcript variant 1	1.36E-02	3.2
SYT4	synaptotagmin IV	1.17E-02	3.1
SYT13	synaptotagmin XIII	2.77E-02	3.1
NCAN	neurocan	1.98E-05	2.7
FGF13	fibroblast growth factor 13, transcript variant 1	2.49E-02	2.6
GDA	guanine deaminase	3.04E-02	2.6
SV2B	synaptic vesicle glycoprotein 2B, transcript variant 1	2.53E-02	2.5
CADPS	Ca++-dependent secretion activator, transcript variant 3	2.98E-03	2.5
BASP1	brain abundant, membrane attached signal protein 1	9.23E-03	2.5
MAL2	mal, T-cell differentiation protein 2	2.84E-02	2.5
GNLY	granulysin, transcript variant NKG5	1.72E-03	2.5
KCNC2	potassium voltage-gated channel, Shaw-related subfamily, member 2, transcript variant 1	4.97E-02	2.5
KCNMA1	potassium large conductance calcium-activated channel, subfamily M, alpha member 1, transcript variant 1	4.47E-02	2.4
CDH18	cadherin 18, type 2	4.70E-02	2.4
TNFRSF12A	tumor necrosis factor receptor superfamily, member 12A	9.98E-03	2.3
RGS7BP	regulator of G-protein signaling 7 binding protein	3.34E-02	2.3
CBLN2	cerebellin 2 precursor	3.44E-02	2.3
ENC1	ectodermal-neural cortex (with BTB-like domain)	3.03E-02	2.2
PRICKLE1	prickle homolog 1 (Drosophila), transcript variant 1	1.99E-03	2.2
MRAP2	melanocortin 2 receptor accessory protein 2	1.17E-02	2.2
HOPX	HOP homeobox (HOPX), transcript variant 2	1.37E-02	2.2
ELMOD1	ELMO/CED-12 domain containing 1, transcript variant 1	4.36E-02	2.2
FGF12	fibroblast growth factor 12, transcript variant 2	1.92E-02	2.2
CHI3L1	chitinase 3-like 1 (cartilage glycoprotein-39)	3.31E-02	2.1
NCEH1	neutral cholesterol ester hydrolase 1, transcript variant 2	1.20E-02	2.1
GABRB3	gamma-aminobutyric acid (GABA) A receptor, beta 3, transcript variant 1	2.34E-02	2.1
CD83	CD83 molecule, transcript variant 1	9.92E-03	2.1
ISG15	ISG15 ubiquitin-like modifier	2.25E-03	2.1
LRRN3	leucine rich repeat neuronal 3, transcript variant 3	5.48E-03	2.1
ALOX5AP	arachidonate 5-lipoxygenase-activating protein	1.27E-02	2.1
ADORA3	adenosine A3 receptor, transcript variant 1	5.58E-03	2.1
OLR1	oxidized low density lipoprotein (lectin-like) receptor 1 (OLR1)	4.36E-02	2.1
ANO4	anoctamin 4	8.29E-04	2.1
GAP43	growth associated protein 43, transcript variant 2	4.75E-02	2.1

Supplemental Table 3C *(continued)*

Gene symbol	Gene name	Adjusted *p*-value	Fold change
GFRA2	GDNF family receptor alpha 2, transcript variant 1	3.22E-02	2.1
TMEM233	transmembrane protein 233 (TMEM233)	8.27E-03	2.1
MX1	myxovirus (influenza virus) resistance 1, interferon-inducible protein p78 (mouse), transcript variant 2	1.90E-03	2.0
CNR1	cannabinoid receptor 1 (brain), transcript variant 2	1.40E-02	2.0
BEX1	brain expressed, X-linked 1	4.88E-03	2.0
GPR98	G protein-coupled receptor 98, transcript variant 1	1.95E-02	2.0
IFI30	interferon, gamma-inducible protein 30	2.04E-02	2.0

Supplemental Table 3D | Top 50 downregulated genes in chronic active PL-NAWM vs inactive PL-NAWM (comparison II)

Gene symbol	Gene name	Adjusted *p*-value	Fold change
LOC100289290	PREDICTED: Homo sapiens similar to hCG2042717	4.21E-02	0.3
CRLF1	cytokine receptor-like factor 1	2.88E-02	0.3
IGJ	immunoglobulin J polypeptide, linker protein for immunoglobulin alpha and mu polypeptides	2.53E-02	0.3
ABCA6	ATP-binding cassette, sub-family A (ABC1), member 6	2.91E-02	0.3
KANK4	KN motif and ankyrin repeat domains 4	5.65E-06	0.3
ENST00000392423	titin isoform novex-3	1.13E-04	0.4
C21orf130	chromosome 21 open reading frame 130, non-coding RNA	5.99E-03	0.4
ARRDC4	arrestin domain containing 4	6.33E-03	0.4
ENST00000313339	Ankyrin repeat domain-containing protein 18A	3.61E-04	0.4
TSPAN8	tetraspanin 8	1.24E-04	0.4
TTN	titin, transcript variant N2-A	4.23E-03	0.4
ARMC3	armadillo repeat containing 3	4.78E-02	0.4
RBM11	RNA binding motif protein 11	6.76E-05	0.5
FSTL5	follistatin-like 5, transcript variant 1	2.54E-03	0.5
DHCR24	24-dehydrocholesterol reductase	1.34E-03	0.5
C15orf51	chromosome 15 open reading frame 51, non-coding RNA	8.10E-03	0.5
HYDIN	hydrocephalus inducing homolog (mouse), transcript variant 1	5.06E-04	0.5
ANKRD20B	ankyrin repeat domain 20B, non-coding RNA	9.18E-04	0.5
POU2AF1	POU class 2 associating factor 1	1.04E-02	0.5
MTUS1	microtubule associated tumor suppressor 1, transcript variant 2	6.76E-05	0.5
PPEF1	protein phosphatase, EF-hand calcium binding domain 1, transcript variant 1	1.62E-02	0.5
MBOAT1	membrane bound O-acyltransferase domain containing 1	3.09E-03	0.5
RELL1	RELT-like 1, transcript variant 1	6.64E-05	0.5
DPYSL5	dihydropyrimidinase-like 5	9.35E-04	0.5
LOC728449	Putative uncharacterized protein ENSP00000334090	7.27E-03	0.5
HN1L	hematological and neurological expressed 1-like	1.15E-03	0.5
TNFRSF21	tumor necrosis factor receptor superfamily, member 21	7.39E-03	0.5
ANKRD18A	PREDICTED: Homo sapiens ankyrin repeat domain 18A	1.00E-03	0.5
SNX24	sorting nexin 24	5.52E-04	0.5
SPARC	secreted protein, acidic, cysteine-rich (osteonectin)	4.14E-02	0.6
GOLGA8E	golgi autoantigen, golgin subfamily a, 8E	9.58E-03	0.6
LOC283481	hypothetical protein	7.39E-03	0.6
AK058117	cDNA FLJ25388 fis, clone TST02351	8.65E-03	0.6
ENST00000423618	Ankyrin repeat domain-containing protein 18B	1.10E-04	0.6
TTC25	tetratricopeptide repeat domain 25	4.52E-02	0.6
LOC645321	PREDICTED: Homo sapiens hypothetical LOC645321	1.05E-02	0.6
MRO	maestro, transcript variant 1	1.28E-03	0.6
KLK6	kallikrein-related peptidase 6, transcript variant B	8.19E-03	0.6
LOC284232	ankyrin repeat domain 20 family, member A2 pseudogene, non-coding RNA	1.44E-02	0.6
RND2	Rho family GTPase 2	8.65E-03	0.6
LRAT	lecithin retinol acyltransferase (phosphatidylcholine--retinol O-acyltransferase)	3.02E-03	0.6
NIPAL4	NIPA-like domain containing 4	9.58E-03	0.6
DNAJC15	DnaJ (Hsp40) homolog, subfamily C, member 15	1.07E-02	0.6

Supplemental Table 3D *(continued)*

Gene symbol	Gene name	Adjusted *p*-value	Fold change
CCDC11	coiled-coil domain containing 11	5.52E-03	0.6
HAPLN2	hyaluronan and proteoglycan link protein 2	2.53E-02	0.6
OFD1	oral-facial-digital syndrome 1	2.52E-03	0.6
MAP4	microtubule-associated protein 4, transcript variant 4	1.95E-02	0.6
CFH	complement factor H, transcript variant 2	1.72E-03	0.6
DNAH12	dynein, axonemal, heavy chain 12, transcript variant 1	3.34E-02	0.6
MOBKL2B	MOB1, Mps One Binder kinase activator-like 2B (yeast)	3.86E-02	0.6

Supplemental Table 3E | Top 50 upregulated genes in chronic active PL-NAWM vs control WM (comparison III)

Gene symbol	Gene name	Adjusted *p*-value	Fold change
GPNMB	glycoprotein (transmembrane) nmb	7.40E-06	7.1
SERPINA3	serpin peptidase inhibitor, clade A (alpha-1 antiproteinase, antitrypsin), member 3	7.76E-04	7.0
APOC1	apolipoprotein C-I	3.21E-08	6.3
VIM	vimentin	1.07E-06	5.1
MSR1	macrophage scavenger receptor 1	1.64E-04	4.8
CD44	CD44 molecule (Indian blood group)	2.31E-03	4.5
OLR1	oxidized low density lipoprotein (lectin-like) receptor 1	4.86E-06	4.2
PALLD	palladin, cytoskeletal associated protein, transcript variant 2	5.95E-06	4.1
CHI3L1	chitinase 3-like 1 (cartilage glycoprotein-39)	2.63E-03	4.0
ANXA1	annexin A1	3.34E-02	3.9
EMP1	epithelial membrane protein 1	9.09E-03	3.8
S100A10	S100 calcium binding protein A10	1.72E-03	3.8
RFTN1	raftlin, lipid raft linker 1	6.08E-04	3.6
IFI30	interferon, gamma-inducible protein 30	2.08E-03	3.5
ANO6	anoctamin 6	2.46E-05	3.5
CP	ceruloplasmin (ferroxidase)	4.50E-04	3.5
ABCA1	ATP-binding cassette, sub-family A, member 1	5.18E-04	3.4
FPR3	formyl peptide receptor 3	1.34E-03	3.3
PLA2G7	phospholipase A2, group VII (platelet-activating factor acetylhydrolase, plasma)	6.16E-04	3.3
CD84	CD84 molecule	4.39E-05	3.3
TGFB2	transforming growth factor, beta 2, transcript variant 2	6.46E-05	3.1
FRMD3	FERM domain containing 3	4.76E-04	3.1
S100A6	S100 calcium binding protein A6	3.39E-05	3.1
NSL1	NSL1, MIND kinetochore complex component, homolog (S. cerevisiae), transcript variant 1	7.01E-11	3.0
LGALS3	lectin, galactoside-binding, soluble, 3, transcript variant 1	7.15E-05	3.0
SAMSN1	SAM domain, SH3 domain and nuclear localization signals 1	2.81E-03	3.0
MS4A7	membrane-spanning 4-domains, subfamily A, member 7, transcript variant 1	4.51E-02	3.0
COLEC12	collectin sub-family member 12	3.71E-04	2.9
DTNA	dystrobrevin, alpha, transcript variant 3	1.26E-04	2.9
FGF2	fibroblast growth factor 2 (basic)	3.16E-05	2.9
NCF2	neutrophil cytosolic factor 2, transcript variant 1	7.06E-03	2.9
SPP1	secreted phosphoprotein 1, transcript variant 1	1.58E-02	2.9
MAFB	v-maf musculoaponeurotic fibrosarcoma oncogene homolog B (avian)	1.78E-02	2.8
SORBS1	sorbin and SH3 domain containing 1, transcript variant 3	1.75E-05	2.8
DST	dystonin, transcript variant 1eB	8.96E-09	2.8
PTPRC	protein tyrosine phosphatase, receptor type, C, transcript variant 1	3.79E-04	2.8
DAAM1	dishevelled associated activator of morphogenesis 1	2.10E-04	2.8
DDR2	discoidin domain receptor tyrosine kinase 2, transcript variant 1	6.43E-05	2.8
TRIM34	tripartite motif-containing 34, transcript variant 3	1.10E-05	2.7
S1PR3	sphingosine-1-phosphate receptor 3	1.06E-03	2.7
DENND2D	DENN/MADD domain containing 2D	1.20E-02	2.7
TPST1	tyrosylprotein sulfotransferase 1	1.80E-04	2.6
MAN2A1	mannosidase, alpha, class 2A, member 1	2.32E-03	2.6

Supplemental Table 3E *(continued)*

Gene symbol	Gene name	Adjusted *p*-value	Fold change
CNN3	calponin 3, acidic	2.26E-03	2.6
MAN1C1	mannosidase, alpha, class 1C, member 1	2.33E-03	2.6
CCRL2	chemokine (C-C motif) receptor-like 2, transcript variant 1	3.69E-04	2.6
EVI2B	ecotropic viral integration site 2B	1.55E-04	2.5
LIMS1	LIM and senescent cell antigen-like domains 1	5.63E-06	2.5
GPR65	G protein-coupled receptor 65	1.17E-02	2.5
SLC5A3	solute carrier family 5 (sodium/myo-inositol cotransporter), member 3	1.13E-03	2.5

Supplemental Table 3F | Top 50 downregulated genes in chronic active PL-NAWM vs control WM (comparison III)

Gene symbol	Gene name	Adjusted *p*-value	Fold change
AL050203	cDNA DKFZp586F1123 (from clone DKFZp586F1123)	1.05E-13	0.1
DEFA3	defensin, alpha 3, neutrophil-specific	9.85E-04	0.1
LOC100132168	hypothetical LOC100132168	7.01E-12	0.2
MYH7B	myosin, heavy chain 7B, cardiac muscle, beta	4.31E-13	0.2
ENST00000443002	DNA-directed RNA polymerases I, II, and III subunit	7.85E-16	0.2
CPAMD8	C3 and PZP-like, alpha-2-macroglobulin domain containing 8	1.46E-02	0.2
YJEFN3	YjeF N-terminal domain containing 3, nuclear gene encoding mitochondrial protein	2.02E-04	0.3
ATPGD1	ATP-grasp domain containing 1, transcript variant 1	3.26E-07	0.3
CIRBP	cold inducible RNA binding protein, transcript variant 2	3.03E-10	0.3
KCNQ2	potassium voltage-gated channel, KQT-like subfamily, member 2, transcript variant 5	5.84E-03	0.3
A_33_P3253832	Unknown	5.69E-06	0.3
ABCA2	ATP-binding cassette, sub-family A (ABC1), member 2, transcript variant 1	1.51E-11	0.3
CITED4	Cbp/p300-interacting transactivator, with Glu/Asp-rich carboxy-terminal domain, 4	1.67E-08	0.3
UNC84B	unc-84 homolog B (C. elegans)	5.56E-10	0.3
LOC283999	hypothetical protein LOC283999	1.49E-17	0.3
LIPE	lipase, hormone-sensitive (LIPE)	1.97E-07	0.3
ENST00000369123	Chromosome 6 open reading frame 220 Fragment	1.30E-06	0.3
CERCAM	cerebral endothelial cell adhesion molecule	2.30E-04	0.3
ENST00000293201	Putative myosin-XVB (Unconventional myosin-15B)(Myosin XVBP)	1.08E-08	0.3
LOC349114	hypothetical LOC349114 (LOC349114), non-coding RNA	1.75E-12	0.3
KLC2	kinesin light chain 2, transcript variant 2	5.17E-05	0.3
ENST00000405068	Exocyst complex component 7 (Exocyst complex component Exo70)	3.64E-08	0.3
DNAJB2	DnaJ (Hsp40) homolog, subfamily B, member 2, transcript variant 1	5.08E-13	0.3
ADORA1	adenosine A1 receptor, transcript variant 1	2.94E-12	0.3
LOC340335	cDNA FLJ23879 fis, clone LNG13743	4.79E-05	0.3
CCDC85B	coiled-coil domain containing 85B	9.80E-09	0.3
A_33_P3209176	Unknown	3.01E-05	0.3
ENST00000371623	Prostaglandin-H2 D-isomerase Precursor (EC 5.3.99.2)	2.18E-16	0.3
PCBP4	poly(rC) binding protein 4, transcript variant 4	1.53E-17	0.3
STMN4	stathmin-like 4	2.68E-02	0.3
CMTM5	CKLF-like MARVEL transmembrane domain containing 5, transcript variant 3	1.02E-08	0.3
TMEM63A	transmembrane protein 63A	4.41E-08	0.3
DAO	D-amino-acid oxidase (DAO)	8.86E-03	0.3
HMX1	H6 family homeobox 1	9.00E-09	0.3
A_33_P3277805	Unknown	1.52E-02	0.3
LTBP3	latent transforming growth factor beta binding protein 3, transcript variant 2	1.57E-10	0.3
DOHH	deoxyhypusine hydroxylase/monooxygenase, transcript variant 2	1.67E-07	0.3
FTCD	formiminotransferase cyclodeaminase, transcript variant A	4.36E-05	0.3
ST3GAL4	ST3 beta-galactoside alpha-2,3-sialyltransferase 4	5.47E-10	0.3
FLJ45445	hypothetical LOC399844, non-coding RNA	1.57E-10	0.3
PAQR6	progestin and adipoQ receptor family member VI, transcript variant 1	1.19E-10	0.3
tcag7.907	hypothetical LOC402483 (FLJ45340), non-coding RNA	2.99E-03	0.3
PNPLA7	patatin-like phospholipase domain containing 7, transcript variant 1	6.75E-07	0.3

Supplemental Table 3F *(continued)*

Gene symbol	Gene name	Adjusted *p*-value	Fold change
LONP1	lon peptidase 1, mitochondrial, nuclear gene encoding mitochondrial protein	3.62E-15	0.3
SBF1	SET binding factor 1	1.30E-10	0.3
ENST00000401999	hypothetical LOC401357	1.52E-09	0.3
HES6	hairy and enhancer of split 6 (Drosophila), transcript variant 1	6.99E-13	0.3
AGAP3	ArfGAP with GTPase domain, ankyrin repeat and PH domain 3, transcript variant 2	9.13E-07	0.3
ATP6V0E2	ATPase, H+ transporting V0 subunit e2, transcript variant 1	1.14E-07	0.3
MVD	mevalonate (diphospho) decarboxylase	2.19E-15	0.3

Supplemental Table 4 | Gene ontology clusters

Term	GO class	Count	Total	*p*-value
Cluster 1				
biological process				
ion transport	GO:0006811	46	732	3.46E-03
cell junction	GO:0030054	28	370	3.46E-03
small GTPase mediated signal transduction	GO:0007264	29	397	3.83E-03
sphingomyelin catabolic process	GO:0006685	3	3	6.40E-03
transport	GO:0006810	109	2317	7.90E-03
localization	GO:0051179	123	2718	1.11E-02
monovalent inorganic cation transport	GO:0015672	22	298	1.19E-02
establishment of localization	GO:0051234	110	2401	1.37E-02
cellular component				
microtubule	GO:0005874	18	203	4.48E-03
anchoring collagen	GO:0030934	4	9	1.19E-02
synaptic vesicle	GO:0008021	8	49	1.38E-02
molecular function				
purine ribonucleotide binding	GO:0032555	82	1580	3.83E-03
ribonucleotide binding	GO:0032553	82	1580	3.83E-03
MAP-kinase scaffold activity	GO:0005078	3	3	6.40E-03
purine nucleotide binding	GO:0017076	83	1650	6.95E-03
passive transmembrane transporter activity	GO:0022803	26	371	1.10E-02
channel activity	GO:0015267	26	371	1.10E-02
GTPase activator activity	GO:0005096	15	168	1.10E-02
ion channel activity	GO:0005216	25	354	1.13E-02
substrate specific channel activity	GO:0022838	25	362	1.38E-02
GTPase activity	GO:0003924	15	175	1.42E-02
Cluster 2				
biological process				
immune system process	GO:0002376	50	715	3.39E-09
immune response	GO:0006955	39	544	2.25E-07
cell proliferation	GO:0008283	42	691	4.14E-05
response to external stimulus	GO:0009605	35	571	3.67E-04
developmental process	GO:0032502	118	2889	3.69E-04
hematopoiesis	GO:0030097	17	154	3.69E-04
immune system development	GO:0002520	18	173	3.69E-04
hematopoietic or lymphoid organ development	GO:0048534	17	165	7.32E-04
regulation of cell proliferation	GO:0042127	28	437	7.87E-04
anatomical structure development	GO:0048856	81	1861	1.28E-03
organ development	GO:0048513	53	1090	2.07E-03
response to wounding	GO:0009611	24	381	5.16E-03
regulation of multicellular organismal process	GO:0051239	18	252	5.49E-03
defense response	GO:0006952	29	505	6.36E-03
positive regulation of cell proliferation	GO:0008284	16	216	6.94E-03
system development	GO:0048731	66	1521	7.91E-03

immune effector process	GO:0002252	11	97	7.91E-03
B cell activation	GO:0042113	8	54	1.03E-02
cell death	GO:0008219	38	757	1.03E-02
death	GO:0016265	38	757	1.03E-02
regulation of immune system process	GO:0002682	10	86	1.03E-02
cell activation	GO:0001775	14	186	1.07E-02
inflammatory process	GO:0006954	18	271	1.07E-02
cytoskeletal protein binding	GO:0008092	23	385	1.07E-02
regulation of programmed cell death	GO:0043067	27	482	1.07E-02
programmed cell death	GO:0012501	36	716	1.21E-02
negative regulation of programmed cell death	GO:0043069	15	210	1.24E-02
nucleosome positioning	GO:0016584	3	5	1.29E-02
myeloid cell differentiation	GO:0030099	9	75	1.29E-02
response to stress	GO:0006950	44	940	1.36E-02
chemotaxis	GO:0006935	12	130	1.37E-02
taxis	GO:0042330	12	130	1.37E-02
multicellular organismal development	GO:0007275	82	2068	1.49E-02
apoptosis	GO:0006915	35	710	1.85E-02
regulation of apoptosis	GO:0042981	26	477	1.85E-02
B cell receptor signaling pathway	GO:0050853	3	6	1.98E-02
cell morphogenesis	GO:0000902	23	408	2.13E-02
cellular structure morphogenesis	GO:0032989	23	408	2.13E-02
regulation of immune response	GO:0050776	9	84	2.13E-02
response to virus	GO:0009615	9	84	2.13E-02
adaptive immune response	GO:0002250	8	69	2.48E-02
adaptive immune response based on somatic recombination of immune receptors built from immunoglobulin superfamily domains	GO:0002460	8	69	2.48E-02
production of molecular mediator of immune response	GO:0002440	5	26	2.58E-02
regulation of binding	GO:0051098	5	26	2.58E-02
regulation of biological process	GO:0050789	141	4043	2.63E-02
cellular developmental process	GO:0048869	65	1598	2.63E-02
cell differentiation	GO:0030154	65	1598	2.63E-02
cell growth	GO:0016049	13	167	2.63E-02
leukocyte mediated immunity	GO:0002443	8	71	2.63E-02
positive regulation of immune response	GO:0050778	8	72	2.76E-02
negative regulation of mast cell cytokine production	GO:0032764	2	2	2.76E-02
regulation of germinal center formation	GO:0002634	2	2	2.76E-02
negative regulation of apoptosis	GO:0043066	14	208	2.81E-02
negative regulation of biological process	GO:0048519	46	1046	2.86E-02
positive regulation of immune system response	GO:0002684	8	73	2.86E-02
cell development	GO:0048468	47	1076	2.87E-02
regulation of cell size	GO:0008361	13	172	2.98E-02
positive regulation of biological process	GO:0048518	43	967	3.01E-02
immunoglobulin production	GO:0002377	4	17	3.01E-02
chitin catabolic process	GO:0006032	3	8	3.01E-02
N-acetylglucosamine catabolic process	GO:0006046	3	8	3.01E-02
regulation of mRNA stability	GO:0043488	3	8	3.01E-02
chitin metabolic process	GO:0006030	3	8	3.01E-02

chitinase activity	GO:0004568	3	8	3.01E-02
regulation of RNA stability	GO:0043487	3	8	3.01E-02
positive regulation of B cell proliferation	GO:0030890	3	8	3.01E-02
biological regulation	GO:0065007	152	4458	3.01E-02
regulation of cell motility	GO:0051270	7	59	3.07E-02
response to chemical stimulus	GO:0042221	26	506	3.19E-02
anatomical structure morphogenesis	GO:0009653	42	947	3.34E-02
regulation of biological quality	GO:0065008	35	753	3.55E-02
regulation of developmental process	GO:0050793	14	217	3.83E-02
regulation of locomotion	GO:0040012	7	62	3.83E-02
amino sugar catabolic process	GO:0046348	3	9	3.86E-02
glycosamine catabolic process	GO:0006043	3	9	3.86E-02
regulation of B cell proliferation	GO:0030888	3	9	3.86E-02
locomotion	GO:0040011	7	63	3.96E-02
leukocyte activation	GO:0045321	12	164	4.47E-02
erythrocyte differentiation	GO:0030218	5	33	4.57E-02
locomotory behavior	GO:0007626	12	165	4.60E-02
negative regulation of immune system process	GO:0002683	3	10	4.81E-02
regulation of Rho GTPase activity	GO:0032319	3	10	4.81E-02
negative regulation of cytokine production during immune response	GO:0002719	2	3	4.81E-02
negative regulation of production of molecular mediator of immune response	GO:0002701	2	3	4.81E-02
cellular component				
basement membrane	GO:0005604	9	63	6.94E-03
extracellular matrix part	GO:0044420	10	95	1.49E-02
plasma membrane part	GO:0044459	69	1681	1.71E-02
plasma membrane	GO:0005886	106	2859	2.13E-02
proteinaceous extracellular matrix	GO:0005578	18	304	3.01E-02
cytoplasm	GO:0005737	180	5493	4.81E-02
molecular function				
protein binding	GO:0005515	214	6395	9.65E-03
actin binding	GO:0003779	18	265	9.77E-03
GTPase binding	GO:0051020	9	71	1.07E-02
small GTPase binding	GO:0031267	7	63	3.96E-02
transcription corepressor activity	GO:0003714	9	103	4.78E-02
mannosyl-oligosaccharide mannosidase activity	GO:0015924	3	10	4.81E-02
signal transducer activity	GO:0004871	77	2039	4.81E-02
molecular transducer activity	GO:0060089	77	2039	4.81E-02
lipopolysaccharide binding	GO:0001530	2	3	4.81E-02

Cluster 4				
biological process				
antigen processing and presentation of peptide or polysaccharide antigen via MHC class II	GO:0002504	10	16	2.06E-16
immune response	GO:0006955	27	544	1.25E-15
antigen processing and presentation	GO:0019882	12	53	3.06E-14
immune system response	GO:0002376	28	715	4.07E-14
response to biotic stimulus	GO:0009607	13	242	1.36E-07
defense response	GO:0006952	17	505	3.24E-07

response to other organism	GO:0051707	11	177	4.36E-07
multi-organism process	GO:0051704	13	279	5.08E-07
response to virus	GO:0009615	8	84	1.83E-06
inflammatory response	GO:0006954	9	271	1.08E-03
humoral immune response	GO:0006959	5	65	1.42E-03
antigen processing and presentation of peptide antigen via MHC class I	GO:0002474	3	12	1.49E-03
response to wounding	GO:0009611	10	381	2.51E-03
antigen processing and presentation of peptide antigen	GO:0048002	3	15	2.85E-03
response to external stimulus	GO:0009605	11	571	1.34E-02
response to chemical stimulus	GO:0042221	10	506	1.87E-02
response to stress	GO:0006950	13	940	4.02E-02
cellular component				
MHC protein complex	GO:0042611	11	33	6.17E-15
MHC class II protein complex	GO:0042613	9	15	6.17E-15
plasma membrane part	GO:0044459	33	1681	1.35E-12
lysosome	GO:0005764	12	179	5.49E-08
lytic vacuole	GO:0000323	12	179	5.49E-08
vacuole	GO:0005773	12	199	1.51E-07
plasma membrane	GO:0005886	39	2859	1.87E-07
integral to plasma membrane	GO:0005887	20	1152	1.28E-05
intrinsic to plasma membrane	GO:0031226	20	1168	1.75E-05
lysosomal membrane	GO:0005765	5	45	3.10E-04
membrane	GO:0016020	56	6035	4.39E-04
vacuolar membrane	GO:0005774	5	54	7.01E-04
vacuolar part	GO:0044437	5	56	7.46E-04
membrane part	GO:0044425	47	5112	4.80E-03
integral to membrane	GO:0016021	42	4488	9.50E-03
intrinsic to membrane	GO:0031224	42	4509	1.05E-02
pigment granule	GO:0048770	4	83	3.49E-02
melanosome	GO:0042470	4	83	3.49E-02
molecular function				
MHC class II receptor activity	GO:0032395	4	7	2.24E-06
signal transducer activity	GO:0004871	26	2039	7.46E-04
molecular transducer activity	GO:0060089	26	2039	7.46E-04
receptor activity	GO:0004872	21	1607	3.38E-03
IgG binding	GO:0019864	2	6	1.43E-02
tumor necrosis factor binding	GO:0043120	2	9	3.14E-02
C-X-C chemokine binding	GO:0019958	2	10	3.54E-02
MHC class I receptor activity	GO:0032393	2	10	3.54E-02

Cluster 5				
biological process				
skeletal development	GO:0001501	3	204	2.81E-02
phosphate transport	GO:0006817	2	87	4.31E-02
cellular component				
collagen type I	GO:0005584	2	3	5.45E-04
fibrillar collagen	GO:0005583	2	11	3.31E-03

extracellular matrix part	GO:0044420	3	95	5.23E-03
collagen	GO:0005581	2	34	1.96E-02
extracellular region part	GO:0044421	5	741	1.96E-02
proteinaceous extracellular matrix	GO:0005578	3	304	4.31E-02
muscle thin filament tropomyosin	GO:0005862	1	4	4.53E-02
microfibril	GO:0001527	1	4	4.53E-02
molecular function				
structural constituent of bone	GO:0008147	2	4	5.45E-04
thyroid hormone transmembrane transporter activity	GO:0015349	1	2	3.51E-02
prothoracicotrophic hormone activity	GO:0018445	1	2	3.51E-02
interleukin-7 binding	GO:0019982	1	2	3.51E-02
interleukin-7 receptor activity	GO:0004917	1	2	3.51E-02
cytokine binding	GO:0019955	2	85	4.31E-02
extracelluar matrix structural constituent	GO:0005201	2	87	4.31E-02
Cluster 6				
biological process				
sterol biosynthetic process	GO:0016126	2	32	4.30E-02
plasminogen activation	GO:0031639	1	1	4.65E-02
steroid biosynthetic process	GO:0006694	2	74	4.65E-02
sterol metabolic process	GO:0016125	2	80	4.65E-02
molecular function				
squalene monooxygenase activity	GO:0004506	1	1	4.65E-02
Rap guanyl-nucleotide exchange factor activity	GO:0017034	1	2	4.65E-02

Clusters are specified in Figure 2. Count= number of significantly regulated genes within GO class; Total= total number of genes within GO class.

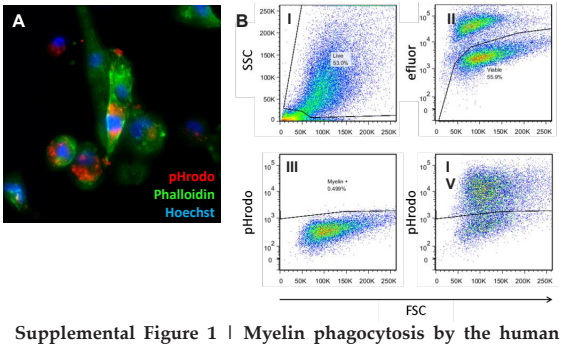

Supplemental Figure 1 | Myelin phagocytosis by the human macrophage cell line THP-1. A) pHrodo-labeled myelin emits a red fluorescent signal upon phagocytosis. For immunocytochemistry, Hoechst was used to stain the nucleus, and phalloidin was used to stain the actin and visualize the cell morphology. **B)** Histograms showing myelin uptake (pHrodo-positivity) in the viable cell population (eFluor-negative) analyzed by flow cytometry. Debris was excluded based on particle size in panel I. Panel I-III: sample without myelin added; panel IV: sample with pHrodo-labelled myelin. FSC=forward scatter; SSC=side scatter. Scale bar in A=50 μm.

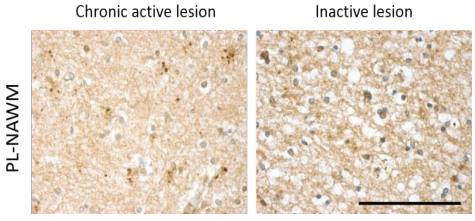

Supplemental Figure 2 | Protein expression of ANO4 at the perilesional site of a chronic active MS lesion. Immunohistochemical staining of ANO4 around chronic active and inactive lesions shows a punctate staining pattern that is more explicit around chronic active lesions. Scale bar = 100 μm.